NBSIR 77-1287

Analytical and Experimental Study of Evaporative Cooling and Room Fire Suppression by Corridor Sprinkler System

Stanley T. Liu

Center for Fire Research
Institute for Applied Technology
National Bureau of Standards
Washington, D.C. 20234

October 1977

Final Report

Supported in Part by:
Office of Policy Development and Research
Department of Housing and Urban Development
Washington, D.C. 20410

NBSIR 77-1287

ANALYTICAL AND EXPERIMENTAL STUDY OF EVAPORATIVE COOLING AND ROOM FIRE SUPPRESSION BY CORRIDOR SPRINKLER SYSTEM

Stanley T. Liu

Center for Fire Research
Institute for Applied Technology
National Bureau of Standards
Washington, D.C. 20234

October 1977

Final Report

Supported in Part by
Office of Policy Development and Research
Department of Housing and Urban Development
Washington, D.C. 20410

U.S. DEPARTMENT OF COMMERCE, Juanita M. Kreps, *Secretary*

Dr. Sidney Harman, *Under Secretary*

Jordan J. Baruch, *Assistant Secretary for Science and Technology*

NATIONAL BUREAU OF STANDARDS, Ernest Ambler, *Acting Director*

CONTENTS

	Page
LIST OF FIGURES	iv
SI CONVERSION UNITS	vi
Abstract	1
1. INTRODUCTION	2
2. MATHEMATICAL ANALYSIS	3
2.1. Evaporative Cooling of a Hot Gas Flow by Water Spray	3
2.1.1. Analysis	3
2.1.2. Numerical Results and Discussion	6
2.2. Trajectory of a Liquid Droplet with Evaporation	8
2.2.1. Analysis	8
2.2.2. Numerical Results and Discussion	11
2.2.3. Scaling Criteria for Reduced Scale Model Test	12
3. EXPERIMENTAL STUDY	13
3.1. Preliminary Full-Scale Corridor Sprinkler Test	13
3.1.1. Test Setup and Instrumentation	13
3.1.2. Test Results and Discussion	14
3.1.3. Comparison of Theoretical and Experimental Results	18
3.2. One-Quarter Scale Model Experiment	19
3.2.1. Experimental Apparatus and Instrumentation	19
3.2.2. Test Procedure	19
3.2.3. Comparison of Full-Scale to One-Quarter Scale Results	20
3.2.4. Test Results Using Solid Fuel	21
4. CONCLUSIONS	23
5. REFERENCES	25
APPENDIX - HEAT TRANSFER BY SPRAY EVAPORATION IN A CROSS FLOW	49

LIST OF FIGURES

		Page
Figure 1.	Schematic of One-Dimensional Model for Spray Evaporation Analysis	26
Figure 2.	Dimensionless Temperature Drop Due to Droplet Evaporation.	27
Figure 3.	Variation in Vapor Concentration Due to Droplet Evaporation.	28
Figure 4.	Similarity of Temperature Variation Due to Droplet Evaporation.	29
Figure 5.	Schematic of a Droplet in a Cross Wind	29
Figure 6.	Trajectory of a Droplet Injected Against a Cross Flow.	30
Figure 7.	Time History of the Variations of a Droplet in High Temperature Cross Flow	31
Figure 8.	Comparison of Droplet Trajectory Based on Scaling Criteria	32
Figure 9.	Schematic of Full-Scale Corridor Sprinkler Test Setup.	33
Figure 10.	Location of Thermocouples, Gas Sampling Port, and Burner (Full-Scale Test)	34
Figure 11.	Time History of Exit Gas Temperature at Burn-room Doorway (No Spray)	35
Figure 12.	Variations of Ceiling Gas Temperature Along the Corridor (No Spray)	36
Figure 13.	Time History of Corridor Ceiling Gas Temperature (0.05 m below Ceiling)	37
Figure 14.	Time History of Corridor Exit Gas Temperature Outside Spray Zone (0.31 m below Ceiling).	38
Figure 15.	Burner Room O_2 and CO_2 Concentration (Floor Level) Just Before the End of Each Run	39
Figure 16.	Comparison of Net Corridor Exit Gas Temperature Reduction by Water Spray (Theoretical vs Experimental).	40
Figure 17.	Schematic of One-Quarter Scale Model Experiment Setup.	41
Figure 18.	Location of Burners, Thermocouples, Gas Sampling Port, and Fuel Pad (One-Quarter Scale Model)	42
Figure 19.	Time History of Corridor Temperature Drop.	43
Figure 20.	Corridor Exit Temperature Reduction, Full-Scale vs One-Quarter Scale Tests.	44

LIST OF FIGURES, cont'd

Figure 21. Burn-room Floor Level Oxygen Content, Full-Scale vs One-Quarter Scale Tests 45

Figure 22. Burn-room Doorway Exit Gas Temperature Variation (Plexiglass Fuel) 46

Figure 23. O_2 Content at Burn-room Floor Level (Plexiglass Fuel) . . . 47

Figure 24. O_2 Content and Gas Temperature Variations (Wood Crib Fuel).. 48

SI CONVERSION UNITS

In view of present accepted practice in this technological area, U.S. customary units of measurement have been used in this report. It should be noted that the U.S. is a signatory to the General Conference on Weights and Measures which gave official status to the metric SI system of units in 1960. Readers interested in making use of the coherent system of SI units will find conversion factors in ASTM Standard Metric Practice Guide, ASTM Designation E 380-72 (available from American Society for Testing and Materials, 1916 Race Street, Philadelphia, Pa. 19103). Conversion factors for units used in this paper are:

Length

1 in = 0.0254 meter

1 ft = 0.3048 meter

Area

$1\ in^2 = 6.4516 \times 10^{-4}\ meter^2$

$1\ ft^2 = 9.2903 \times 10^{-2}\ meter^2$

Pressure

1 psi = 6895 pascal

Volume

$1\ gal = 3.785\ dm^3$

Density of Water Application

$1\ gal/min/ft^2 = 40.746\ mm/min$

ANALYTICAL AND EXPERIMENTAL STUDY OF EVAPORATIVE COOLING AND ROOM FIRE SUPPRESSION BY CORRIDOR SPRINKLER SYSTEM

Stanley T. Liu

Abstract

Investigations, both theoretical and experimental, are conducted to evaluate the effects of a corridor sprinkler system on the cooling and suppression of a fire in an adjacent compartment connected by an open doorway. A simplified one dimensional mathematical model is presented to predict the net reduction of the corridor ceiling hot gas temperature by evaporative cooling. Scaling criteria based on the analysis of the motion of an evaporating droplet were developed for the correlation of full-scale and small-scale experimental results and the design requirements of a small-scale experiment. Representative test results from a full-scale and a one-quarter scale model experiments are presented. These tests demonstrate the effectiveness of water spray in reducing the corridor hot gas temperature to a level low enough for safe passage, and in causing a strong recirculating flow at the room doorway. This flow reduces the oxygen content around the fire significantly, and results in a much reduced burning rate of the fuel. The effect of the spray droplet size on the cooling and on fire suppression is discussed.

Key words: Automatic sprinklers; compartment fire; corridor sprinkler systems; droplet size; droplet trajectory; evaporative cooling; fire suppression; full-scale test; gas temperature; oxygen content; recirculating flow; reduced scale model test; scaling criteria; spray water flow rate; water spray.

1. INTRODUCTION

In October 1973, the U.S. Department of Housing and Urban Development (HUD) issued changes to fire protection requirements in the Minimum Property Standards (MPS) for multi-family [1][1] and Care Type [2] Housing. These changes pertained to the installation of automatic sprinklers in these occupancy types. Of particular interest was the requirement for installation of automatic sprinklers in corridors in all multi-family structures four stories or more in height and in care-type housing of fire resistive or noncombustible construction regardless of height. In March 1974, a research project, sponsored by the Office of Policy Development and Research of HUD, was initiated at the National Bureau of Standards (NBS) to evaluate the current criteria [3] and to improve design for corridor sprinkler systems. This report, as part of the overall project, is a study on the function and effectiveness of using water spray in the corridor when there is a fire in an adjacent compartment with the door left open. The objectives are to study (1) the cooling of the hot combustion products issuing out of the doorway by the evaporation of the spray droplets and, (2) the containment and possible extinguishment of the fire in its room of origin.

In general, the water spray from a sprinkler works to contain and suppress a fire underneath it by direct wetting and cooling of the combustibles, by evaporative cooling of the hot combustion products above the combustibles, and by returning the oxygen deficient upper atmosphere down to the region around the burning fuel. This is discussed in some detail in reference [4]. For the spray to be effective, a network of sprinklers is generally installed directly above the combustibles to be protected. For the present study where the water spray is outside the burn-room, direct wetting of the burning combustibles is insignificant. However, another mechanism, the transfer of momentum between the spray and the hot gas flow exiting from the doorway and along the corridor ceiling, comes into play. This transfer of momentum from the spray droplets to the hot gas flow caused by aerodynamic drag on the droplets creates a downward motion of the gas flow toward the corridor floor. This flow has a very low oxygen concentration because it contains the original products of combustion, vapor from the droplets, and partly evaporated droplets. When this flow comes into contact, mixes with, and is carried by the floor level fresh air inflow back into the burn-room, oxygen supply to the room is reduced. The amount of reduction in oxygen

---

[1] Numbers in brackets refer to the literature references listed at the end of this paper.

concentration determines the decrease in the burning rate of the fuel and the possible extinguishment of the fire. This complex process depends on the effectiveness of droplet evaporation and momentum transfer, which in turn are dependent on the water spray flux-density and droplet diameter, and is the subject of the study here.

In this report, both a mathematical analysis and some experimental results will be presented. The mathematical analysis will be presented in two parts. The first part will be a study on the effects of spray droplet diameter on the cooling of a hot gas flow as it travels down the length of the corridor under a simplified one dimensional geometry. The second part will study the momentum transfer and change in the trajectory of a droplet as it is injected into a hot gas flow. A scaling criteria for relating full-scale and small-scale experiments based on the analyses will be presented. The experimental study involves both full-scale and one-quarter scale model tests. Results and observations of these tests including the fire behavior, the corridor ceiling gas temperature variations, and the burn-room floor level oxygen and carbon dioxide concentrations, all under the action of the water spray from sprinklers and spray nozzles, will be shown.

2. MATHEMATICAL ANALYSIS

2.1. Evaporative Cooling of a Hot Gas Flow by Water Spray

2.1.1. Analysis

Previous investigations on the heat and mass transfer of fine liquid droplets in a gaseous medium were conducted mostly by researchers in the combustion research field and in the spray-drying industry. A summary of their works are given together with a comprehensive list of references in a review paper by Bahn [5] and more recently by Masters [6] and Ahmadzadeh and Harker [7]. Both theoretical and experimental works were reported. Part of their findings, which has a direct bearing upon the present study, are summarized as following:

(1) During evaporation, the droplet temperature remains constant and is equal to the adiabatic saturation temperature of the surrounding hot gas at temperature T and humidity ω. For an air-water-vapor system, the adiabatic saturation temperature is the same as the wet-bulb temperature.

(2) For droplets with diameter less than 1.5 mm, the effects of surface circulation and volume distortion can be neglected and the droplets can be treated as solid spheres.

(3) For air-water-vapor system at 1 atm pressure, the Lewis Number (ratio of Prandtl Number and Schmidt Number) is close to 1. An analogy between heat transfer and mass transfer exists, and the Nusselt Number for heat transfer can be estimated by using the Ranz-Marshall correlation [8]:

$$Nu_D = hD/k_a = 2\,(1 + 0.3\,Re_D^{1/2}\,Pr^{1/3}) \qquad (1)$$

where

Nu_D = Nusselt Number based on droplet diameter = hD/k_a

h = Convection heat transfer coefficient

D = Droplet diameter

k_a = thermal conductivity of air

Re_D = Reynolds Number based on droplet diameter = UD/ν

Pr = Prandtl Number of air = ν/α

ν = Kinematic viscosity of air

α = Thermal diffusivity of air

The analysis described here deals with the case of hot combustion products flowing out of a compartment door into a corridor where a water spray directed normal to the gas flow acts to continuously reduce the gas temperature along the length of the corridor by evaporation. To simplify the analysis, a one-dimensional model is used, and air is assumed to be the gas.

The simplified model is shown in figure 1. Hot dry air at temperature T_o and mass flow rate $\dot{m}_a$ is assumed to exit from a door and rise immediately up to the ceiling. The hot air moves down the corridor with a flow area of WxH where W is the width of the corridor and H the depth below the ceiling. Water spray with a uniform droplet diameter D at a given height and uniform droplet flux density $\dot{N}$ flows vertically down from the ceiling through the hot air layer at a constant terminal velocity V_t and temperature T_s. Cold air at temperature T_a is assumed to be underneath the hot air layer and flows in the opposite direction. Stable stratification, hence no mixing, is assumed for this analysis.

The following additional assumptions are made:

(1) Airflow is turbulent with uniform velocity and temperature at any location x.

(2) All the corridor surfaces are adiabatic and the only heat transfer is between the hot air and the water droplets. Radiation is neglected, and no mixing occurs between the hot and cold air layers. Preheating of the droplets from their initial temperature to the wet-bulb temperature T_s is also neglected when compared with the heat of evaporation.

(3) Mixing of the hot air and the vapor generated by evaporation is instantaneous. Vapor assumes the same velocity and temperature as the airflow.

By writing down the mass balance and energy balance equations for a differential control element dx at x, and applying equation (1), the change in the hot air temperature and the water vapor mass flow rate along the length of the corridor due to the evaporation of the spray is shown to be (details of the derivation are shown in the appendix) in dimensionless form:

$$\frac{B(\theta - 1)}{1 + B\theta} - (1 + B) \ln \left[\frac{\theta(1+B)}{1 + B\theta} \right] = ES \qquad (2)$$

$$\omega(S) = B \, (cp_a/cp_v) \, (1 - \theta) \qquad (3)$$

where

$\theta = (T-T_s)/(T_o - T_s)$ = Dimensionless temperature

$\omega = \dot{m}_v/\dot{m}_a$ = humidity ratio

$S = X/W$ = Dimensionless distance along the corridor

$B = cp_v \, (T_o-T_s)/h_{fg}$ = Spalding's B Number for evaporation (4)

$E = (\pi D^2 N W^2 H h)/(\dot{m}_a \, cp_a \, V_t)$ = $\frac{\text{Total heat transferred to droplets}}{\text{Energy input}}$

$\dot{N}$ = Droplet flux density (No. of droplets/sec/unit area normal to spray flow)

$\dot{m}_v$ = Mass flow rate of vapor

h_{fg} = Latent heat of evaporation at T_s

cp_v, cp_a = Specific heat of vapor and air, respectively

h = heat transfer coefficient to a droplet, from eq. (1)

In obtaining eqs. (2) and (3), the heat transfer coefficient h was assumed to remain constant. This is not actually true since the droplet diameter and the terminal velocity are continuously decreasing when falling through the hot air layer, and h is a function of the diameter and velocity (Reynolds Number). To estimate the variation of h as a function of temperature and droplet diameter, a calculation was made for h at three temperature levels and three droplet sizes covering the ranges normally encountered in actual conditions, and is shown in the following table:

T_o	T_s	Values of Heat Transfer Coeff. h in $J/s \cdot m^2 \cdot K$ for Droplet Diameter of		
°C	°C	1 mm	1/2 mm	1/4 mm
600	85	329	414	607
280	60	283	346	482
120	35	272	323	443

where T_o is the hot air inlet temperature and T_s is the adiabatic saturation temperature of the water droplets. Values of T_s for the values of T_o shown are experimental data given in reference [9]. Physical property values of air (c_{pa}, k_a, ν,α) were evaluated at the arithmatic mean of T_o and T_s. Since the fraction change in droplet diameter is proportional to 1/3 power of the change in mass, the decrease in droplet diameter is much smaller than the decrease in mass. For example, a reduction of the droplet mass by evaporation to one-half of its original value will reduce the droplet diameter by only 20%. For a 1 mm diameter droplet at constant T_o, this will result in a change in the value of h by less than 6% as computed from equation 1. Since a normal sprinkler produces droplets with diameter mostly in the range of 0.5 mm to 1.2 mm where evaporation is not very efficient [10], the assumption of a constant value for h is a reasonable assumption for estimation purpose.

2.1.2. Numerical Results and Discussion

Numerical examples of eqs. (2) and (3) are computed for the values of T_o, T_s, and D listed in the above table for h. Computations were based on the following data:

$$\dot{m}_a = .545 \text{ kg/s}$$

Spray water volume flux density = .0339 $dm^3/s \cdot m^2$ (.05 $gal/min \cdot ft^2$)

$$H = 1.22 \text{ m}$$

$$W = 2.44 \text{ m}$$

The value of $\dot{m}_a$ is equivalent to the hot gas mass flow rate of a fully-developed room fire. The spray flux density is approximately equal to a flow rate of 1.262 dm^3/s (20 gal/min) from a sprinkler head with a coverage of 37.16 m^2 (400 ft^2) at a distance of 1.22 m (4 ft) underneath the sprinkler head [10]. The results are shown in figures 2 and 3.

Figure 2 shows the effect of droplet diameter on the variation of the dimensionless mixture temperature due to droplet evaporation versus the dimensionless corridor distance S. It is seen that for droplets with diameter larger than 0.5 mm, a long length of corridor is required to reduce the mixture temperature to a low level. Since the droplet diameter varies in some fashion directly with the nozzle diameter of a sprinkler for the same water flow rate, the installation or design using a small orifice sprinkler is indicated. Figure 3 shows the variations of the mixture humidity ratio as an indication of the total amount of evaporation. It is seen that, for the purpose of cooling, spray with a large droplet diameter (larger than 0.5 mm) is not very efficient. This is in agreement with the conclusion presented in reference [10].

It should be pointed out that in obtaining the above results, heat loss through the walls and the mixing of hot and cold air layers were neglected. Both of these act to decrease the temperature along the corridor in addition to the decrease caused by evaporation. Therefore, in an actual situation, a sprinkler which gives a spray with mean droplet diameter as large as 1 mm might be satisfactory as far as cooling of the combustion products down the corridor is concerned. However, for the purpose of vapor generation and recirculation as a means of fire suppression, droplets with smaller diameter are preferred. This will be shown later in the results from the full-scale tests.

Examination of eq. (2) shows that if the temperature variation θ is plotted versus the product ES, all the curves in figures 2 and 3 will approximately merge into a single curve for all expected values of B (or gas inlet

temperature). This is shown in figure 4. Therefore, the parameter E acts as a stretching factor and can be used as a scaling factor for scale model experiments.

2.2. Trajectory of a Liquid Droplet with Evaporation

2.2.1. Analysis

The motion of a droplet in a high temperature gas medium has been studied in reference [10] in determining the distance of penetration of the droplet into a rising hot gas plume. There the ability of the droplet in penetrating the rising plume is the main criterion, and the motion of the droplet was assumed to be one-dimensional and in the vertical gravitational plane. The present study deals with the motion of an evaporating droplet injected at an arbitrary angle into a horizontal high temperature gas stream. The objective is to obtain information on:

(1) the maximum distance of throw of a droplet in a spray as a function of the droplet diameter when injected opposing to a hot ceiling gas flow,

(2) the change in the trajectory of the droplet so as to quantify the momentum transfer between the droplet and the hot gas flow, and

(3) the scaling criteria needed in correlating reduced scale experimental results with full-scale tests.

The study is restricted to the two-dimensional case, that is, the motion of the droplet is in a vertical plane parallel with the streamline of the hot gas flow.

A schematic of the problem is shown in figure 5. A droplet with initial diameter D_o and velocity U_o at temperature T_s is injected at at angle θ_o into a horizontal hot air stream at velocity V_a and temperature T_a. The wet-bulb temperature of the air stream is equal to the droplet temperature T_s.

Applying Newton's second law of motion to the droplet in the horizontal and vertical directions, results in,

Horizontal: $$m \frac{du_x}{dt} = F_D \sin\phi \qquad (5)$$

Vertical: $$m \frac{du_y}{dt} = -F_D \cos\phi + mg\,(1 - \rho_a/\rho_w) \quad (6)$$

where $$\phi = \tan^{-1}(u_x - V_a)/u_y \quad (7)$$

$$F_D = \text{Drag force} = C_D\,(\tfrac{1}{2} A_j \rho_a U^2) \quad (8)$$

U = relative velocity of droplet to airstream

$$U^2 = (u_x - V_a)^2 + u_y^2 \quad (9)$$

$$u = (u_x^2 + u_y^2)^{1/2} = \text{droplet velocity} \quad (10)$$

$$C_D = \text{drag coefficient} = C\,Re_D^{-1/2} \quad (11)$$

$$m = \tfrac{1}{6} \pi \rho_w D \quad (12)$$

$$A_j = \tfrac{1}{4} \pi D^2 = \text{Projected area of droplet} \quad (13)$$

ρ_w, ρ_a = density of water and air, respectively .

The evaporation rate of the droplet in flight is,

$$-\frac{dm}{dt} = hA\,(T_a - T_s)/h_{fg} \quad (14)$$

where $A = \pi D^2$ = surface area of the droplet,

h_{fg} = latent heat of evaporation of water

h = heat transfer coefficient from eq. (1).

The initial conditions for equations (5), (6), and (14) are, at t = 0;

$$u_x = U_o \sin\theta_o$$

$$u_y = U_o \cos\theta_o$$

$$D = D_o$$

The relationship of C_D versus Re_D, eq. (11), with the constant C=12, fits well with the experimental correlation of a sphere [11] for Reynolds Number from 10 to 200 which is the range of interest in the present study. The effects of acceleration and evaporation on C_D are neglected (which was also the assumption used in references 6 to 8).

After re-arrangement of equations (5) to (15), and assuming $(1-\rho_a/\rho_w) = 1$, the equations can be written as, in dimensionless form,

$$\frac{du_x^*}{dt^*} = -(3/4)\, C_{D_o}\, H^* D^{*-3/2}\, (\rho_a/\rho_w)\, f(u_x^*, u_y^*)\,(u_x^*-V_a^*) \tag{16}$$

$$\frac{du_y^*}{dt^*} = -(3/4)\, C_{D_o} H^* D^{*-3/2}\, (\rho_a/\rho_w)\, f(u_x^*, u_y^*)\, u_y^* + \frac{1}{Fr} \tag{17}$$

$$\frac{dD^*}{dt^*} = -2G(H^*/D^*)(Re_o Pr)^{-1}\left[2 + 0.6\, Pr^{1/3} Re_o^{1/2}\, d^{*1/2}\, f(u_x^*, u_y^*)\right] \tag{18}$$

Initial conditions:

$$\text{at } t^* = 0; \qquad u_x^* = \sin\theta_o$$

$$u_y^* = \cos\theta_o$$

$$D^* = 1 \tag{19}$$

where

$$f(u_x^*, u_y^*) = \left[(u_x^*-V_a^*)^2 + u_y^{*2}\right]^{1/4}$$

$$u_x^* = u_x/u_o$$

$$u_y^* = u_y/U_o$$

$$V_a^* = V_a/U_o$$

$$
\begin{aligned}
t^* &= tU_o/H \\
H^* &= H/D_o \\
D^* &= D/D_o \\
C_{D_o} &= 12/Re_o^{1/2} \\
R_{e_o} &= \rho_a U_o D_o/\mu_a \\
Fr &= U_o^2/gH = \text{Froude Number} \\
G &= \rho_a C_{p_a} (T_a - T_s)/(\rho_w h_{fg})
\end{aligned}
\qquad (20)
$$

2.2.2. Numerical Results and Discussion

The system of the three first order non-linear differential equations (16) to (18) has no known closed form solutions, thus numerical solutions using the Runge-Kutta method were obtained for the following conditions:

U_o = 12.2 m/s

V_a/U_o = 0.1

θ_o = -90°

H = 1.22 m

T_a = room temperature (no evaporation), and 600 °C (T_s = 85 °C)

D_o = 1/4, 1/2, 3/4, and 1 mm.

The results of the numerical solution are shown in figures 6 to 8. Figure 6 shows the difference in the trajectory of a droplet with and without evaporation in a high temperature environment. The change in the horizontal distance travelled and the longer time required to travel a certain vertical distance due to the changing diameter by evaporation is clearly shown. For the case D_o = 1/4 mm, the droplet is completely evaporated in less than

0.5 second over a very short distance of vertical fall. For droplet injected at less than 90° angle, the influence of evaporation will be less in a finite thickness hot air layer because of a shorter residence time. Note that the curving trajectory of the droplet in the cross airflow gives an indication of the blocking effect of a large group of droplets on the airflow caused by the transfer of momentum from the decelerating droplets to the airflow. The circles in the figure indicate the position of the droplet at each 0.1 second interval.

Figure 7 shows the percent change in droplet diameter, mass, and magnitude of velocity as a function of time. It is seen that the smaller the diameter the faster the rate of change.

2.2.3. Scaling Criteria for Reduced Scale Model Test

Examination of equations (16) and (17) shows that if the droplet diameter is assumed to remain constant, similarity in droplet trajectory will result under the same temperature environment if the following four parameters are kept constant:

$$V_a^* = V_a/U_o = \text{constant}$$

$$Fr = U_o/gH = \text{constant}$$

$$H^*C_{D_o} = \text{constant}$$

$$t^* = t\,U_o/H = \text{constant} \qquad (21)$$

Equations (21) can be used as the scaling criteria when conducting a reduced scale model study. If the length scale ratio of full size to the model is L, eq. (21) will give, for the model,

$$H \sim 1/L$$

$$U_o \sim V_a \sim D_o \sim t \sim 1/L^{1/2} \qquad (22)$$

The mass flow rate of the combustion products is proportional to area times velocity, which gives the scaling of mass flow rate as:

$$\dot{m}_a \sim H^2 V_a \sim 1/L^{5/2} \qquad (23)$$

For the flow field of the full-scale and the model to be similar, the initial momentum ratio of the water spray to the combustion products should be kept constant. Therefore, $\dot{m}_w U_o / \dot{m}_a V_a$ = constant, which gives the scaling of the mass flow rate of the spray as:

$$\dot{m}_w \sim \dot{m}_a \, (V_a/U_o) \sim \dot{m}_a \sim 1/L^{5/2} \tag{24}$$

From previous analysis on the temperature variation of the combustion products flowing through a spray of water droplets, the parameter $E = \pi(\dot{N}D^2 HW^2 h)/(c_{p_a} \dot{m}_a U_o)$ is found to be useful for scaling. Assuming the heat transfer coefficient, h, is constant, the scaling factor for the droplet flux density is by equations (23) and (24),

$$\dot{N} \sim (\dot{m}_a U_o)/(D^2 H^3) \sim L \tag{25}$$

The above relationship for scaling spray droplets was also obtained by G. Heskestad [12].

When the droplet diameter changes due to evaporation, similarity in trajectory no longer holds. However, it still holds in an approximate sense where L is equal to 4. Thus, it is seen from figure 8 that when plotted against the dimensionless time t^*, and scaled droplet diameter $D_o/\sqrt{L}$, the deviations in trajectory are close enough to be acceptable. Equations (22) to (25) therefore can be used as a criterion for reduced scale model study with the scale factor L equal to 4.

3. EXPERIMENTAL STUDY

3.1. Preliminary Full-Scale Corridor Sprinkler Test

3.1.1. Test Setup and Instrumentation

In order to determine qualitatively on an experimental basis the effect of the interaction of the water spray and the hot gas flow on the fire inside the burn-room, a short series of tests was conducted under a simplified burn-room and corridor arrangement. In this arrangement, hexane fuel injected through a nozzle at the floor level was used to simulate the fire in a compartment with door open to a corridor. The burn-room was located at the end of the corridor and in line with the corridor vertical center plane. This is

to provide a simpler flow path for the hot gas of the burn-room in order to avoid the complication of the normal room-corridor situation with a sharp 90° turn and its accompanying complex flow pattern. A schematic of the arrangement is shown in figure 9.

Instrumentation for this special test involved a gas sampling setup with the sampling port located at 0.15 m above the burn-room floor midway between the burner and the burn-room doorway. Two Chromel-Alumel (30 gage) thermocouples were installed inside the burn-room near the ceiling and thirty were installed outside in the corridor along the vertical center-plane at various heights from the floor level. The locations of the burner, gas sampling port, and thermocouples are shown in figure 10. Samples of gas from the burn-room were fed to an electrolytic oxygen detection cell and an infrared carbon dioxide analyzer which continuously monitored the O_2 and CO_2 concentration levels in the air stream going to the burn-room. The thermocouples in the corridor were shielded from direct contact with the spray droplets by shallow cups (24 mm diameter) with the thermocouple bead just clear of the bottom of the cup. This arrangement proved to be fairly successful except for several thermocouples near the centerline of the sprinkler head where droplets carried by strong local circulation wetted the thermocouple bead. These thermocouples then measured the water temperature rather than the gas temperature.

Tests were conducted for a series of different sprinkler sizes, heat release rates, and sprinkler water flow rates. The test conditions are listed in table 1. Each test was run for 150 seconds except for 5 of these tests which lasted only 60 to 75 seconds because the flame was starved out which automatically triggered a safety mechanism and shut off the fuel supply. The sprinkler was turned on manually 25 to 30 seconds after the fire was started in all the tests. A check out run with the automatic release mechanism in place showed that 20 seconds is required for the 74 °C (165 °F) rated sprinklers to open under the fire sizes tested.

3.1.2. Test Results and Discussion

The results of the full-scale tests are shown in table 1, and figures 11 to 15. Table 1 gives the time averaged burn-room hot gas temperature measured 0.31 m below the ceiling. It is interesting to note that the time-averaged burn-room hot gas temperature in some cases is higher than the calibration run with no water spray. This is probably caused by the observed lifting up of the flame and the consequent burning of the fuel at a height closer to the

Table 1. Test Conditions of Full-Scale Corridor Sprinkler Experiment

Test No.	Heat Release* Rate, $\dot{Q}_h$ (kW)	Sprinkler Size (nominal, inch)	Water Flow Rate $\dot{Q}$ (gal/min)	Burn-Room Gas Temperature**, Time Averaged (°C)	Observations and Comments
1	738	Calibration run		610	No water spray
2	738	1/2	24.5	587	Fog fill-in corridor and burn-room
3	738	1/2	20	572	Little fog present
4	738	3/8	20	608	Fog fill-in corridor and burn-room
5	738	3/8	15	602	Some fog
6	738	3/8	10	630	Little fog. Droplets very large
7	738	1/4	15	616	Flame-out in 40 s. Thick fog obscure flame.
8	738	1/4	15	600	Flame-out in 40 s. Thick fog obscure flame
9	738	1/4	10	608	Little fog. Droplets very large
10	350	Calibration run		456	No water spray
11	350	1/2	35	486	Flame-out in 40 s. Thick fog obscure flame
12	350	1/2	30	517	Flame-out in 50 s. Thick fog
13	350	1/2	30	505	Flame lift up. Thick fog.
14	350	1/2	25	502	Some fog.
15	350	3/8	24	512	Flame lift up. Thick fog.
16	350	3/8	20	510	Fog fill-in corridor and burn-room
17	350	3/8	15	490	Some fog.
18	350	1/4	10	488	Little fog.
19	1050	1/4	15	670	Flame-out in 30 s. Thick fog
20***	350	1/4	15	514	Large amount of fog.
21***	738	1/4	15	629	Large amount of fog

*Heat release rates are only approximate values due to inaccuracy in fuel flow rate measurement.

**Measured 0.31 m below ceiling and 0.61 from doorway.

***Sprinkler located 2.75 m from burn-room doorway.

ceiling than the one with no water spray. The heat release rates in table 1 are only a qualitative indication of the fire size due to the inaccuracy in fuel flow measurement. Table 1 also gives a description of visual observation during the tests. In general, whenever the flame was put out, thick fog (condensing vapor) was also present and obscured the view of the flame. This is caused by the large amount of evaporation of the water spray.

Figures 11 and 12 are the results of the two calibration runs without water spray. Figure 11 shows the time history of the burn-room doorway exit gas temperature measured 0.46 m below the doorway soffit. This temperature is a measure of the average initial gas temperature the water spray will contact, and it is seen that it reaches a fairly steady-state after 30 seconds for both fire sizes (indicated by the burn-room gas temperature near the ceiling). The much lower gas temperature at the doorway as compared to the burn-room gas temperature is caused by the large entrainment of incoming cold air into the exit gas layer at the doorway. Figure 12 shows the decrease in the ceiling hot gas temperature measured at 0.05 m below the ceiling as it flows down the corridor due to heat loss through the wall and entrainment of incoming cold air below the hot gas layer, as discussed in section 2.1.2.

Figure 13, 14, and 15 are examples of the results of the tests with the sprinkler turned on. Figure 13 shows a typical case on the temperature variation of the ceiling gas flow before and after the sprinkler operation. It is seen that the temperature was significantly reduced when the sprinkler was turned on. The temperature at 4.5 m from the doorway was reduced to such a low level (60 °C) that heat from the combustion products no longer poses a problem if the corridor is used for evacuation purpose. However, this does not take into account the effect of poisonous smoke in the flow. Since this particular burner used produced very little smoke, the effect of the water spray on the bulk movement of smoke in a fire could not be determined during this series of tests.

Figure 14 shows the effect of the sprinkler size, and hence the spray weight mean droplet diameter, on the corridor ceiling exit gas temperature just outside of the spray zone. The temperature measured was at 0.31 m below the ceiling which is a measure of the average ceiling flow gas temperature. It is seen that for approximately the same water flow rate through the sprinkler head, and at approximately the same temperature level at the time the spray was turned on, the smaller sized sprinkler which produces a spray with a smaller weight mean droplet diameter [10] achieved a larger temperature reduction. This confirms the conclusion of section 2.1.

Figure 15 gives the oxygen and carbon dioxide concentration of the incoming airflow at the floor level (0.15 m above) of the burn-room just before the end of each run. Data from both fire sizes (test Nos. 2-9 and 11-18) are plotted on the graph since, from figure 11 it can be seen that the doorway exit gas temperatures are fairly close for both fire sizes. The normal concentration levels near the burn-room floor are 20.9% for O_2 and 0.1% or less for CO_2, both by volume. An increase in CO_2 level and a decrease in O_2 level indicate the presence of the combustion products and vapor mixture carried down from the ceiling level by the water spray and mixed with the incoming fresh airflow, and the amounts changed give an indication of the strength of the recirculation. It is seen that for the same water flow rate, the smaller orifices which produced smaller weight mean diameter droplets created a stronger recirculation flow. For the four cases where the fire was put out, the concentration level changed drastically, which showed the effectiveness of the blockage of the fresh air inflow by the recirculation flow. It is also seen that the smaller orifice sprinklers required a much smaller water flow rate to produce the required recirculation flow. Therefore, if a sprinkler is to be used for this special type of fire control, it should be designed to give a mean droplet diameter in the 0.5 mm to 1.0 mm range.

The effect of the location of the sprinkler with respect to the burn-room doorway is obtained by comparing the results of test Nos. 7, 20 and 21 (table 1). In test No. 7, the sprinkler was located 1.22 m from the doorway while in tests 20 and 21 it was 2.75 m from the doorway. The comparison is shown in the following table. The data were the results at the end of each test.

	Test 7	Test 20	Test 21
Burn-room % O_2 Concentration (floor level)	17.0	19.3	19.1
Burn-room % Co_2 Concentration (floor level)	2.9	1.10	1.35
Corridor exit gas temperature (4.5 m from doorway)	40 °C	90 °C	110 °C
Fire at end of test (observation)	out	not out	not out

It is seen from the above table that the spray is more effective in creating recirculation flow at the doorway and in reducing the temperature downstream of the corridor when placed closer to the doorway. This is because the spray that covers the doorway encounters the exiting hot gas flow at a higher temperature since there is less chance of heat loss to the walls and mixing of hot and cold gas layers. The higher temperature gradient between the hot gas and the water droplets results in a better evaporation effect. Therefore, it is better to locate the sprinkler closer to the doorway than farther away from it.

3.1.3. Comparison of Theoretical and Experimental Results

An examination of figure 4 shows that, for all expected values of B, the dimensionless temperature θ can be written as, approximately,

$$\theta = (T-T_s)/(T_o-T_s) = f(ES).$$

Re-arranging terms of the above equation gives

$$\Delta T = T_o - T = (T_o-T_s)[1-f(ES)] \qquad (26)$$

where ΔT is the net reduction in the hot gas temperature due to spray evaporation.

Figure 16 shows a comparison of the theoretical results from equation (26) and the experimental results on the reduction of the corridor exit gas temperature. The experimental values are the differences of measured temperatures just before the spray was turned on and just before it was turned off. The values are from the thermocouple located at 0.31 m below the ceiling and just outside of the spray zone. The value T_o in equation (26) was assumed to be 350 °C because an examination of figure 11 and also the data from the runs with the spray on showed that the burn-room doorway exit gas temperature measured at 0.46 m below the soffit were in the range of 325 °C to 360 °C. The weight mean droplet diameters for the three sprinkler sizes, at a flow rate of 0.945 to 1.26 dm^3/s (15 to 20 gpm) and a spray flux density of 0.034 liter/s·m^2 (0.05 gpm/ft^2), were estimated to have a value of between 0.9 mm to 1.2 mm based on experimental results reported in reference [10]. It is seen from figure 16 that the agreement between the theoretical value based on a uniform droplet size, and the experimental results, are fairly good. However, this agreement should be tempered with the fact that the theoretical

model can only be used to predict the net reduction in the hot gas temperature due to spray evaporation. It cannot be used to predict the actual temperature variation of the hot ceiling gas flow without the incorporation into the formulation of the heat loss through the wall and the complex mixing effect of the hot gas and cold air layers.

3.2. One-Quarter Scale Model Experiment

In section 2 of this report, it is seen that it is possible to use a reduced scale model in conducting the experiment discussed in section 3.1. Since a reduced scale model experiment is less costly and less time consuming to conduct and more versatile in varying the parameters associated with a problem in determining their effects on the results, a one-quarter scale (L = 4) burn-room corridor apparatus was constructed. The purpose was to determine whether the scaling criteria developed in section 2 are applicable by comparing the results obtained with the previous full-scale test, and to conduct experiments with different sources of fuel to determine the effects of the water spray on the burning characteristics of the fuels.

3.2.1. Experimental Apparatus and Instrumentation

A schematic of the experimental apparatus is shown in figure 17. A 0.61-m cube burn-room made of 1.27 cm thickness asbestos millboard is connected to a 0.61-m by 0.61-m cross sectional area corridor, 2.14-m long and made of 1/16-inch stainless steel plate. The burn-room and the corridor are separated by a 0.23-m by 0.51-m doorway centered at the centerline of the corridor. Instrumentation involved the measurement of oxygen concentration near the burn-room floor, three thermocouples (gage 30, chromel-alumel) located at the burn-room doorway exit, burn-room floor level, and corridor ceiling exit (outside of spray zone), respectively, and the natural gas and water flow rates to the meeker burners and spray nozzle, respectively. The locations of the burners, gas sampling port, and thermocouples are shown in figure 18. The output from the electrolytic O_2 detector cell and the thermocouples were recorded on strip-chart recorders.

3.2.2. Test Procedure

Tests were conducted using three small industrial spray nozzles of different design to simulate a sprinkler. The three nozzles are, from data obtained from the manufacturers:

1. Pin nozzle where the spray is generated by a solid jet impact on a pin opposing the jet. The weight mean droplet size is in the range of 0.25 to 0.20 mm at a flow rate of 1.01 dm^3/min (0.267 gpm) and at a nozzle pressure of 2.76 x 10^5 pascal, (or 40 psig). The spray included angle is 90°.

2. Spiral nozzle with an included angle of 90° and a flow rate of 1.38 dm^3/min (0.366 gpm) at a nozzle pressure of 2.76 x 10^5 pascal. The weight mean droplet size is approximately 0.3 to 0.4 mm.

3. Whirl nozzle with an included angle of 120° and a flow rate of 1.07 dm^3/min (0.283 gpm) at a nozzle pressure of 2.76 x 10^5 pascal. The weight mean droplet size is approximately 0.4 to 0.5 mm.

Three types of fuel were used during the test. They are:

1. Methane gas through four meeker burners at a total heat release rate of 21 kW,

2. Plexiglass plate 0.635 cm thick and a surface area of 465 cm^2 and 697 cm^2,

3. Small wood cribs with a total mass of 1.75 kg made of 0.65 cm by 0.65 cm wood sticks with a spacing of 0.65 cm.

The tests with methane gas as fuel were run with all three nozzles under steady-state conditions to check the validity of the scaling criteria discussed previously. Steady-state run with meeker burner is possible because the air supply to the burner is through the burner itself by virtue of the design of the meeker burner. The tests with the solid fuel were run with the pin nozzle due to its closer resemblence with a regular sprinkler. The results of the test are discussed in the following paragraphs.

3.2.3. Comparison of Full-Scale to One-Quarter Scale Results

To check the validity of the scaling criteria (eqs. (21) to (25)) described previously, a series of steady-state tests using the meeker burner with methane gas as fuel were conducted. The results of those tests, as compared with the full-scale tests, are given in figures 19 to 21.

Figure 19 shows an example of the time history of the corridor temperature drop when the spray was turned on. With the scale factor L = 4, the scaled water flow rate through the nozzle was $\dot{Q}_w L^{5/2} = 0.775$ dm^3/s (12.3 gpm) (eq. (24)) as compared with the full-scale rate of 0.945 dm^3/s (15 gpm). It is seen that under similar doorway exit gas temperatures, the rate and magnitude of the corridor temperature drop outside the spray zone are very similar for the full-scale and one-quarter scale tests.

Figure 20 shows the net reduction in the corridor exit gas temperature as a function of the scaled water flow rate, and figure 21 shows the change in the oxygen concentration at the burn-room floor level due to the action of the spray. Based on a weight mean droplet diameter of 0.9 mm for the 1/4-in sprinkler for the full-scale, the mean droplet diameter for the small nozzles should be $0.9\ L^{-1/2} = 0.45$ mm which is fairly close to two of the three nozzles tested. It is seen from figure 20 and 21 that the results for the full-scale and one-quarter scale tests agree reasonably well. The smaller net reduction in the corridor exit temperature and the larger decrease in the O_2 content for the one-quarter scale tests are probably caused by the difference in the spray included angle of the nozzles which is 180° for the three sprinklers and 90° to 120° for the small nozzles. Since the hot gas layer is near the ceiling a larger included angle of the spray covers more of the hotter gas layer and gives longer residence time for the spray droplets in the layer. Both tend to improve the effect of evaporation. On the other hand, a smaller angle gives a larger downward momentum transfer from the droplets to the hot gas and hence creates a better recirculation flow.

From the above discussion, it is seen that the one-quarter scale model design based on the scaling criteria of equations (21) to (25) can be used to simulate and predict results of a full-scale test, provided some care is exercised in choosing spray nozzles to simulate the full-scale flow patterns.

3.2.4. Test Results Using Solid Fuel

In the previous test using meeker burners with methane gas as fuel under steady-state conditions, the burning rate of the fuel is independent of the fresh air inflow through the doorway to the burn-room. In an actual room fire, the oxygen content of the burn-room determines the burning rate of the combustibles in the room. To investigate the effect of a corridor water spray on the burning rate and possible extinguishment of a solid fuel, tests were conducted using plexiglass plates and wood cribs located in the back half of the burn-room on a piece of 1.2 cm thickness asbestos millboard

as shown in figure 18. The fuel was ignited with a small amount of alcohol and steady burning over the entire plexiglass surface or the wood cribs was established before the spray was turned on. The pin nozzle was used as the spray nozzle since the pin acts as a deflector and gives a closer resemblance to the deflector in a regular sprinkler. The results of the tests are illustrated in figures 22, 23 and 24.

Figures 22 and 23 show the burn-room doorway exit gas temperature and the burn-room floor level oxygen content variations as a function of time after the spray is turned on. The fuel was plexiglass plate with surface areas of 465 cm^2 and 697 cm^3, respectively. Observation during the tests showed that the flame over the burning surface of the plexiglass was extinguished within 30 seconds for the 697 cm^2 case. For the smaller fuel surface area (465 cm^2) case, the burning area was reduced to less than one-quarter of the original area and restricted to the back edge of the plate, but the burning remained thereafter in a near steady-state. These observations are shown clearly in figures 22 and 23. The burning rate is represented by the doorway exit hot gas temperature and it is seen that in both cases the temperature starts to decrease after the spray is turned on. This decrease in burning rate is caused by a decrease in the oxygen supply to the burning fuel as shown in figure 23. Figures 22 and 23 also show that for the flame to be put out, the initial fire size and hence the exit temperature should be high enough so that enough vapor can be generated and circulated back into the burn-room to reduce the oxygen content around the fuel rapidly enough to a level low enough to starve out the flame. It is interesting to note that even though the flame was not completely extinguished for the smaller fire size, the burning rate remained at a reduced rate even with the oxygen content going back to a near normal level. This is probably because some very small water droplets were carried into the burn-room together with the recirculating flow and either physically wet the fuel surface or absorb enough heat by evaporating around the fuel to keep the burning rate from returning to its original level.

Figure 24 shows the case when wood crib was used as the fire source. Observation during the test again showed that the flame was reduced to only flickering near the back edge of the crib. However, the fire over the whole crib was not extinguished but stayed in a glowing state, even though the burning rate stayed at a much reduced rate. When the spray was turned off, flaming burning returned to the whole crib rapidly as can be seen from figure 24 on the rise of the doorway exit temperature and the burn-room floor level oxygen content in front of the fire. Figure 24 also shows a

typical change of the corridor ceiling gas temperature outside of the spray zone and the temperature near the burn-room floor level in front of the fire. It is seen that the spray actually reduced the corridor exit temperature below that of the incoming air temperature to the burn-room. The increased burn-room floor level air temperature is caused by the mixing of part of the doorway exit hot gas entrained into the spray with the fresh air inflow. This also serves as an indication of the creation of recirculation flow by the spray.

It should be pointed out that the extinguishment of a flaming plexiglass fire is dependent on the size of the burn-room. If the room is much larger than the present one, steady-state burning might be achieved sooner and the room oxygen content will not be decreased to the level required for flame out to occur. However, reduced burning rate will still be achieved as shown in figures 22 to 24. Comparison of the behavior of the fire using the two different types of solid fuel also shows that complete extinguishment of a fire with the corridor spray depends on the type of combustibles in the room. For a fire in an advanced stage like a fully developed deep burning crib fire, smoldering fire will continue even with a much reduced oxygen content in the room. This is similar to the problem in firefighting encountered sometimes when CO_2 is used as an extinguishing agent. Unless the temperature of the entire burning fuel is reduced to a low level, there is the chance of returning to flaming combustion once the application of the extinguishing agent is stopped.

4. CONCLUSIONS

Based on the analysis and experiments described in the previous section, the following conclusions are obtained:

1. It is possible to predict the net reduction in corridor exit gas temperature, when a sprinkler in the corridor is turned on, by a simplified one-dimensional analysis. The analysis shows that spray with a smaller weight mean droplet diameter is more effective in cooling down the hot combustion products.

2. Scaling criteria based on the motion of a single evaporating droplet are developed and shown to be applicable in the design of a reduced scale model experiment and in correlation of the results between the model and full-scale tests.

3. Full-scale and reduced scale model tests show that when a fire is burning in an adjacent room with open doorway, the application of a water spray in the corridor is effective in reducing the corridor exit gas temperature outside of the spray zone to a level low enough for safe passage.

4. It is possible for the spray to create a recirculating flow at the doorway so that vapor, fine droplets, and the combustion products will flow back into the burn-room. This back flow can reduce the burning rate of the fuel to a much lower level, and may even be able to extinguish the fire if the initial fire size is large enough so that sufficient vapor is generated to sufficiently reduce the oxygen content around the fire.

5. A smaller sprinkler that produces a smaller mean droplet size under the same water flow rate is more effective than a larger sprinkler in both the cooling of the combustion products and reducing the burning rate of a fuel.

6. The sprinkler is more effective when placed closer to the doorway than farther away from the doorway.

Finally, it should be pointed out that due to the limited number of test runs and limitation of the nozzle design, the results are only a qualitative indication of the effects of the spray on the hot gas flow and on the fire. Further tests on a more comprehensive plan and with a better design and knowledge of the nozzle characteristics (exact droplet size, spray flux density and larger spray angle) are needed to fully ascertain the optimum droplet size, spray angle, spray flow rate, and the effects of the spray and the limitation on a quantitative basis.

5. REFERENCES

[1] Minimum Property Standards for Multi-family Housing, HUD 4910.1, Department of Housing and Urban Development, Washington, D.C. (1973 Edition).

[2] Minimum Property Standards for Care-Type Housing, HUD 4920.1, Department of Housing and Urban Development, Washington, D.C. (1973 Edition).

[3] Installation of Automatic Sprinkler Systems, NFPA No. 13, National Fire Protection Association, Boston, Mass (1975 Revision).

[4] Thompson, N. J., Fire Behavior and Sprinklers, Chapter 7, National Fire Protection Association, Boston, Mass. (1964).

[5] Bahn, G. S., Role of Vaporization Rate in Combustion of Liquid Fuels, Literature of the Combustion of Petroleum, Advances in Chemistry Series 20, American Chemical Society, Washington, D.C. (1958).

[6] Masters, G., Spray Drying, Chapter 8, CRC Press, The Chemical Rubber Company (1972).

[7] Ahmadzadeh, J. and Harker, J. H., Evaporation from Liquid Droplets in Free Fall, Trans. Inst. Chem. Engrs., Vol. 52 (1974).

[8] Ranz, W. E. and Marshall, W. R., Jr., Evaporation from Drops, Chemical Engineering Progress, Vol. 48, Nos. 3 & 4 (1952).

[9] Nishiwaki, N., Kinetics of Liquid Combustion Processes: Evaporation and Ignition Lag of Fuel Droplets, Fifth Symposium (International) on Combustion, The Combustion Institute (1955).

[10] Yao, C. and Kalelkar, A. S., Effect of Drop Size on Sprinkler Performance, FMRC Series No. 18792 (May 1970).

[11] Schlichting, H., Boundary Layer Theory, 4th Ed., McGraw-Hill Book Co., New York (1960).

[12] Heskestad, G., Physical Modeling of Fire, Journal of Fire and Flammability, Vol. 6 (July 1975).

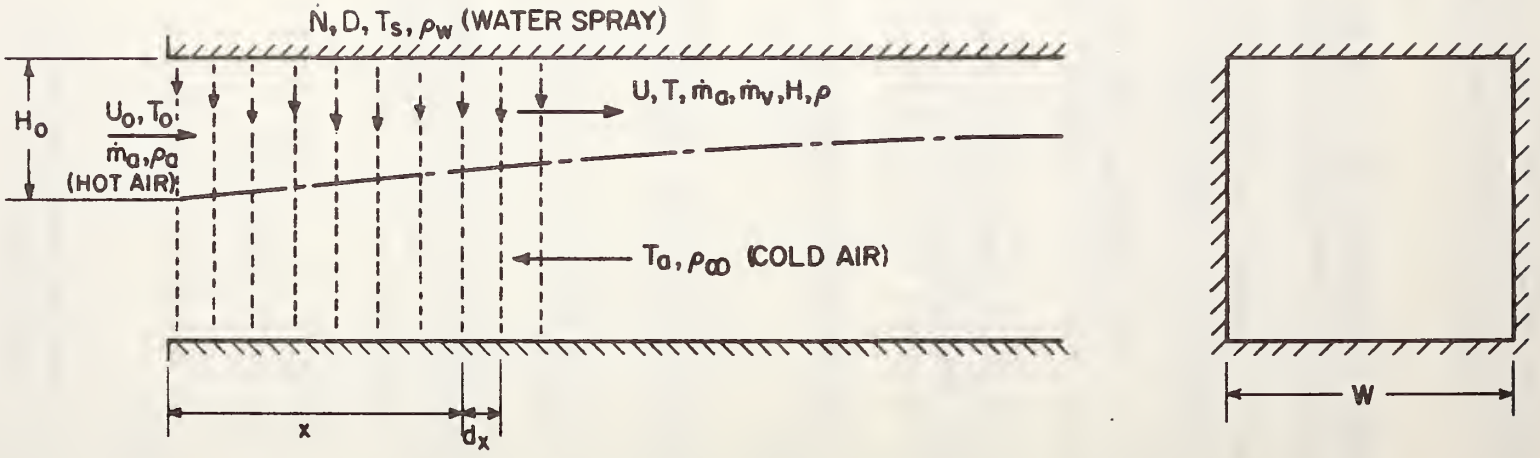

Figure 1. Schematic of One-Dimensional Model for Spray Evaporation Analysis

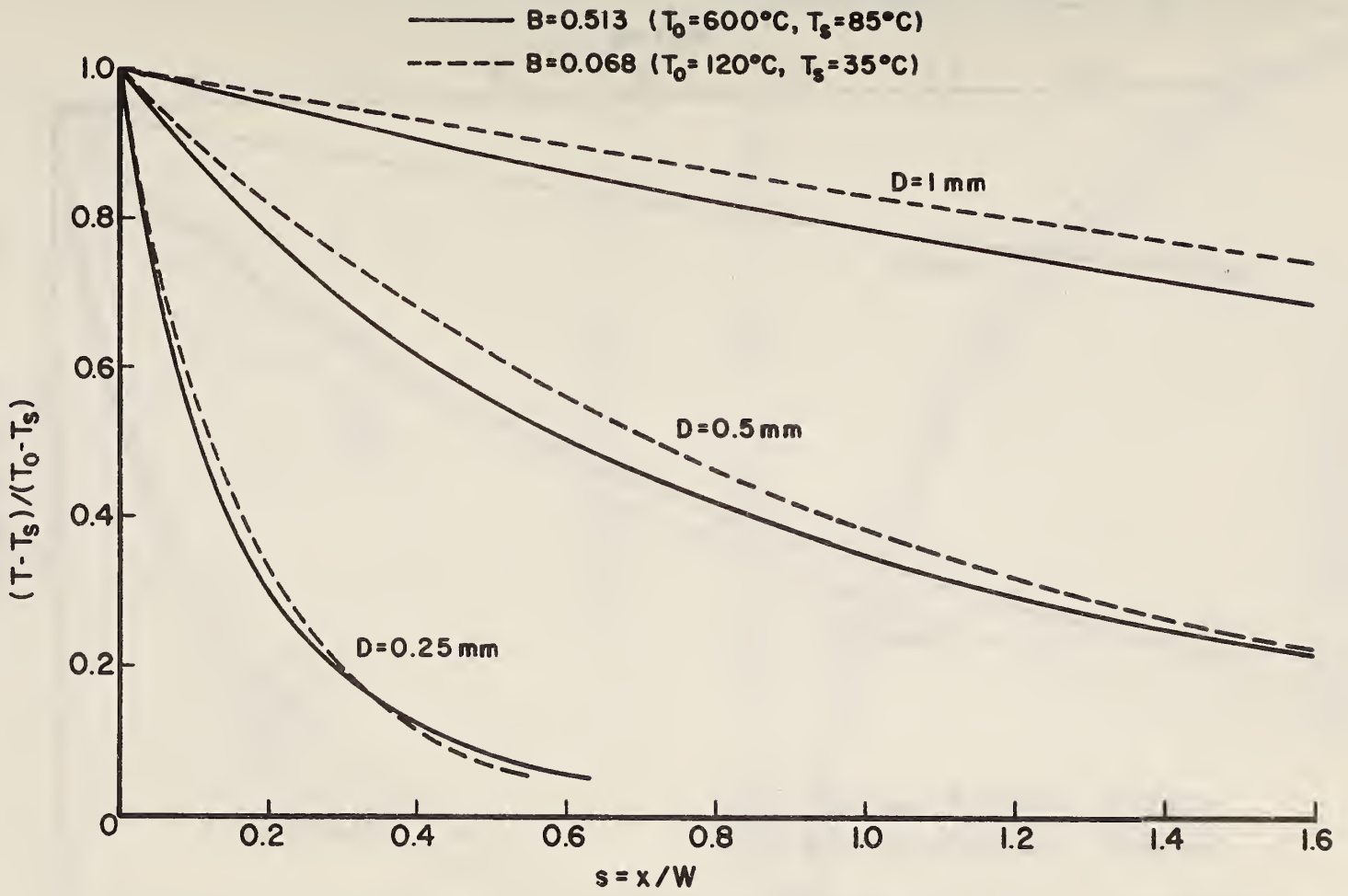

Figure 2. Dimensionless Temperature Drop Due to Droplet Evaporation

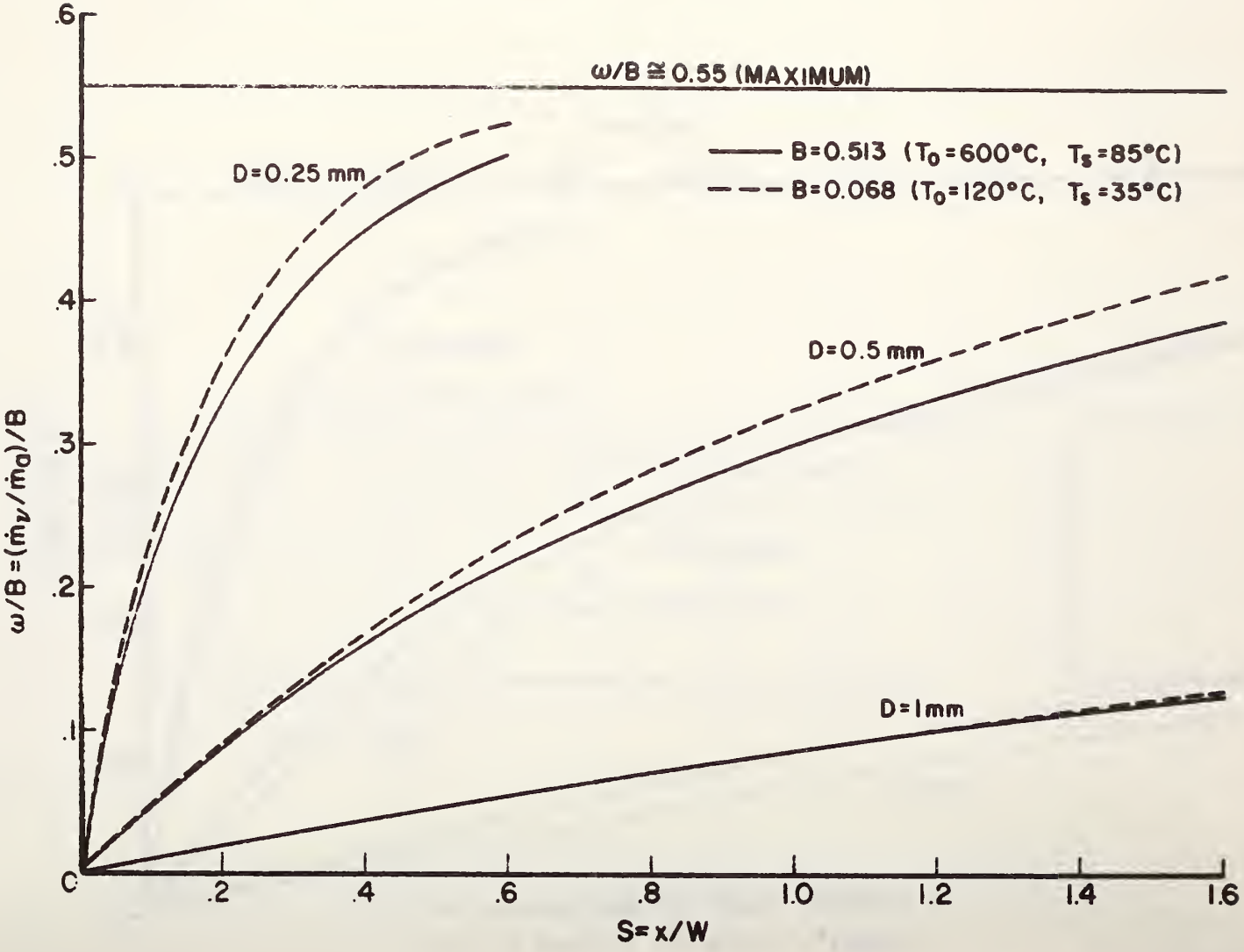

Figure 3. Variation in Vapor Concentration Due to Droplet Evaporation

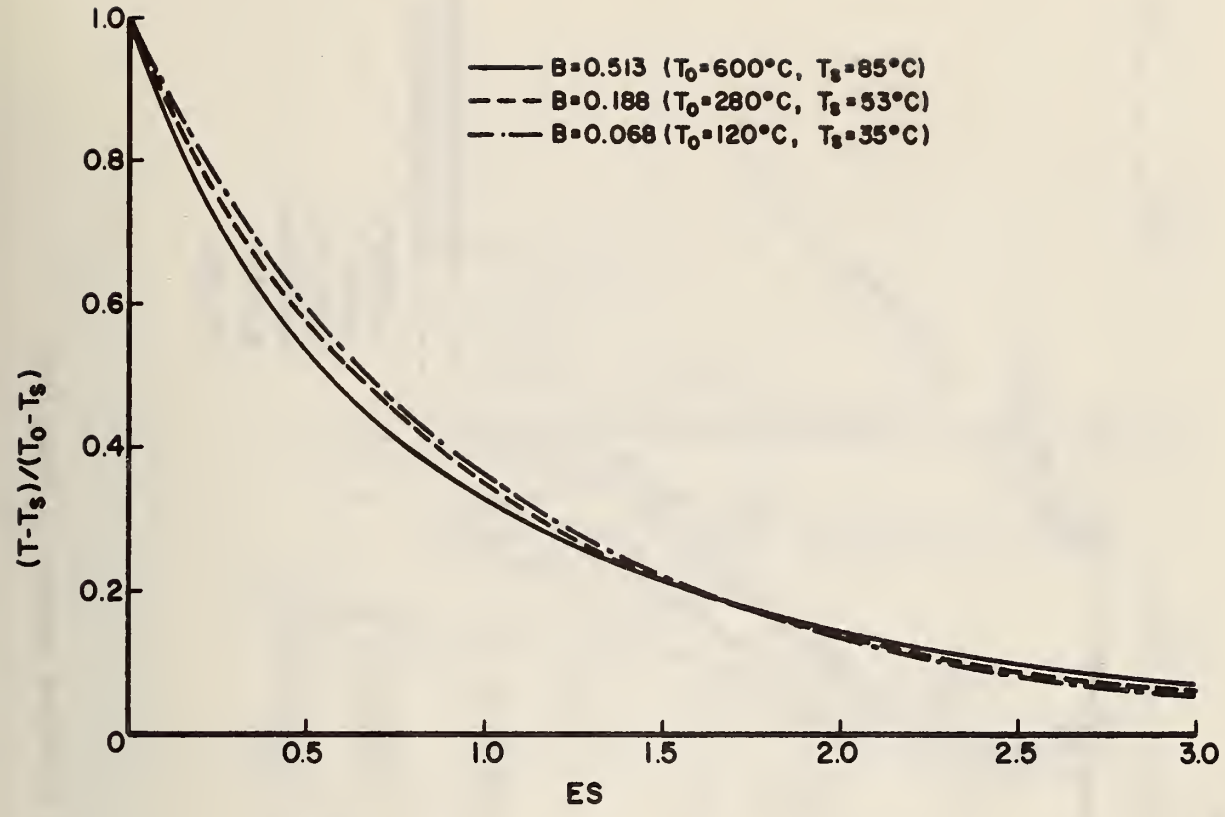

Figure 4. Similarity of Temperature Variation Due to Droplet Evaporation

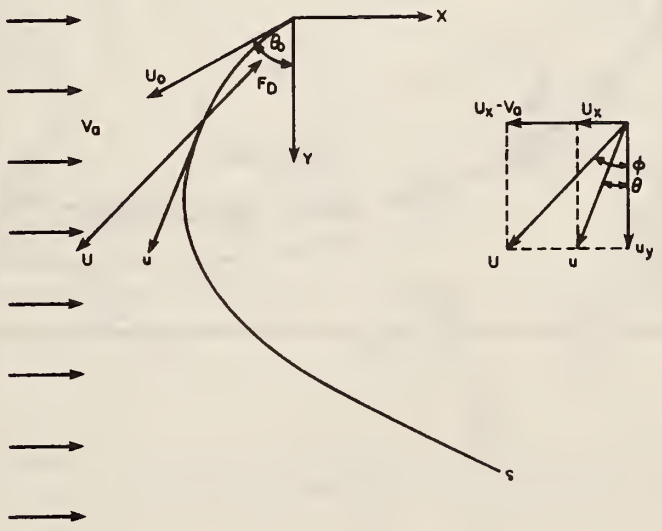

Figure 5. Schematic of a Droplet in a Cross Wind

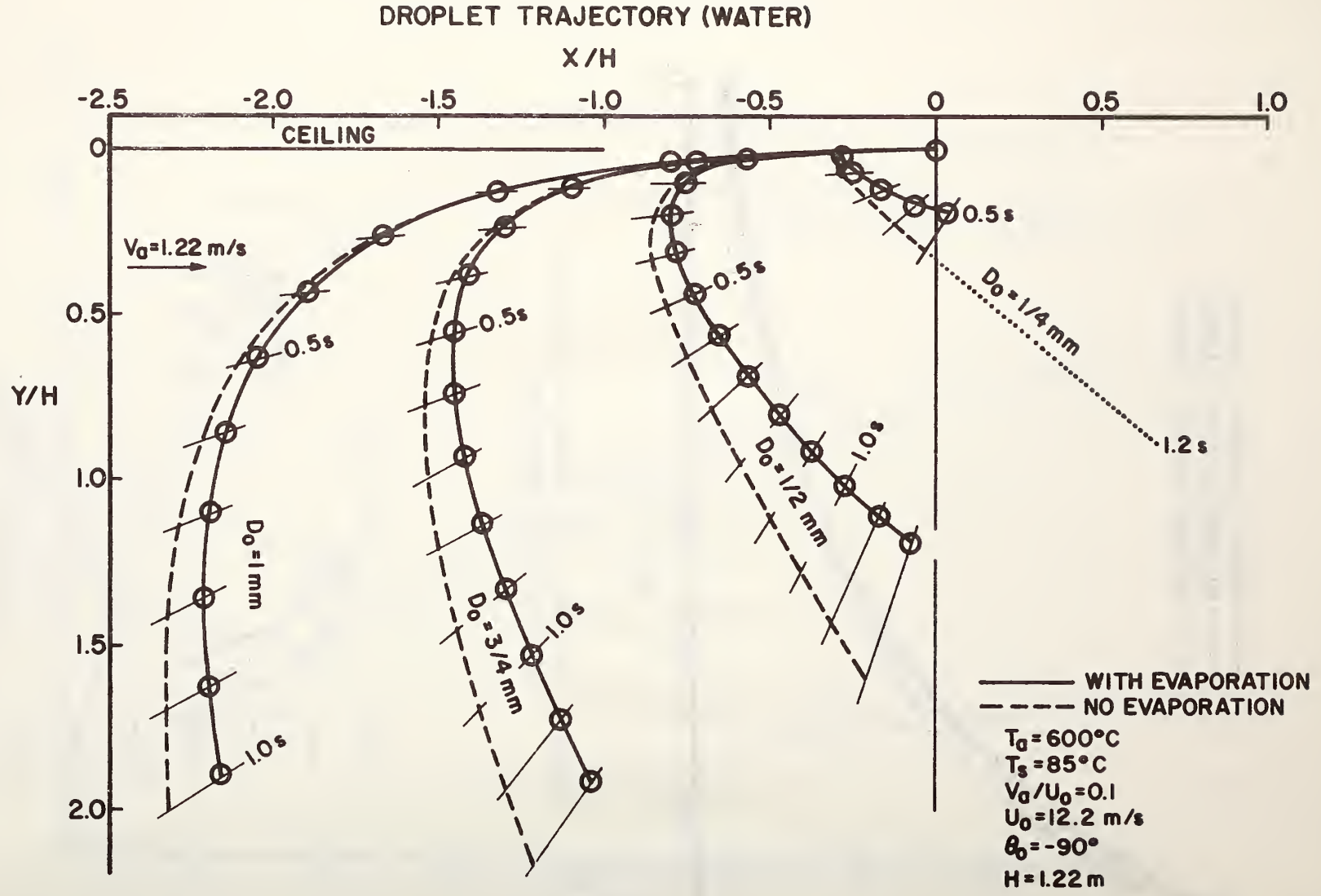

Figure 6. Trajectory of a Droplet Injected Against a Cross Flow

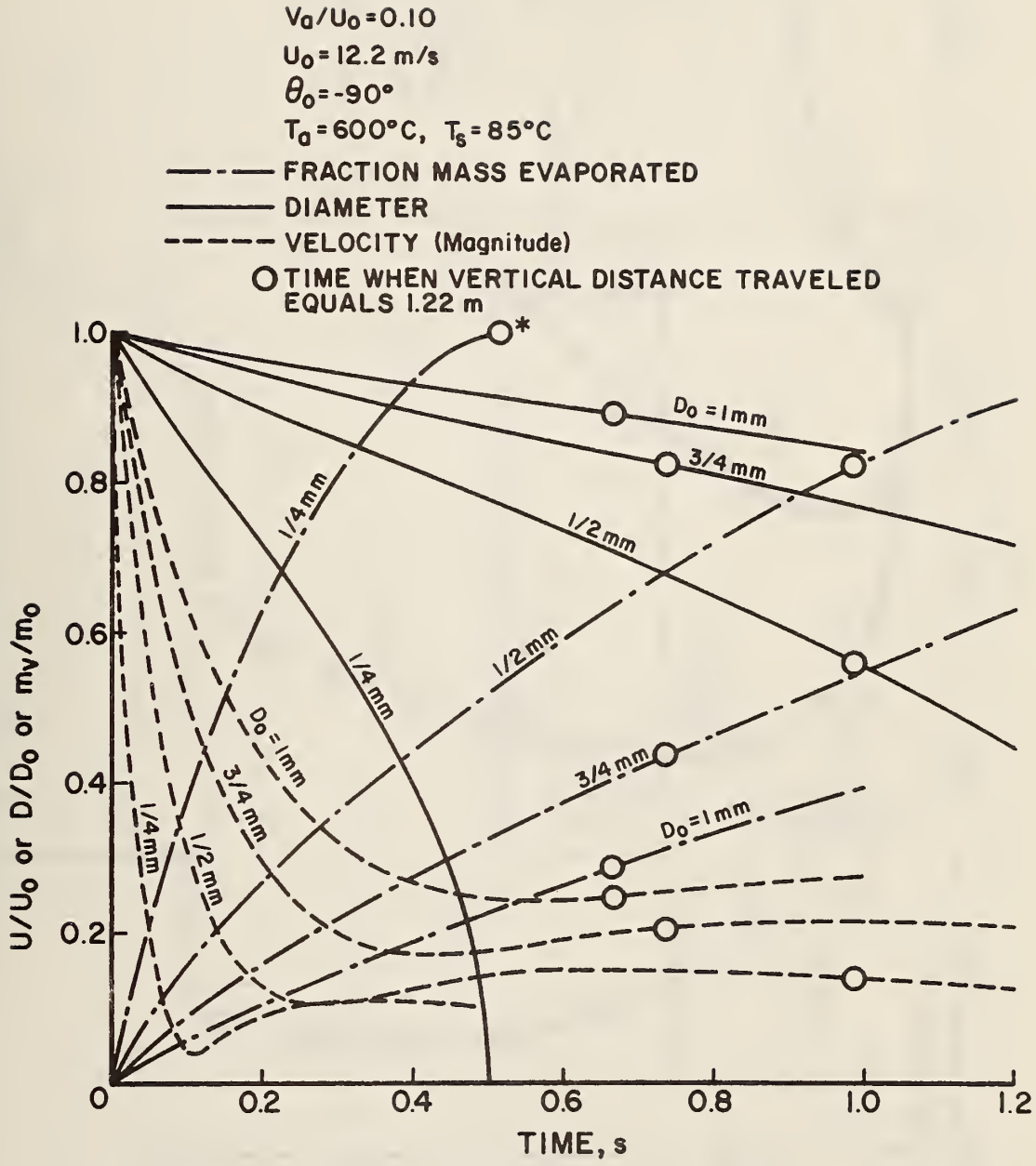

Figure 7. Time History of the Variations of a Droplet in High Temperature Cross Flow
(O* Evaporated Prior to 1.22 m)

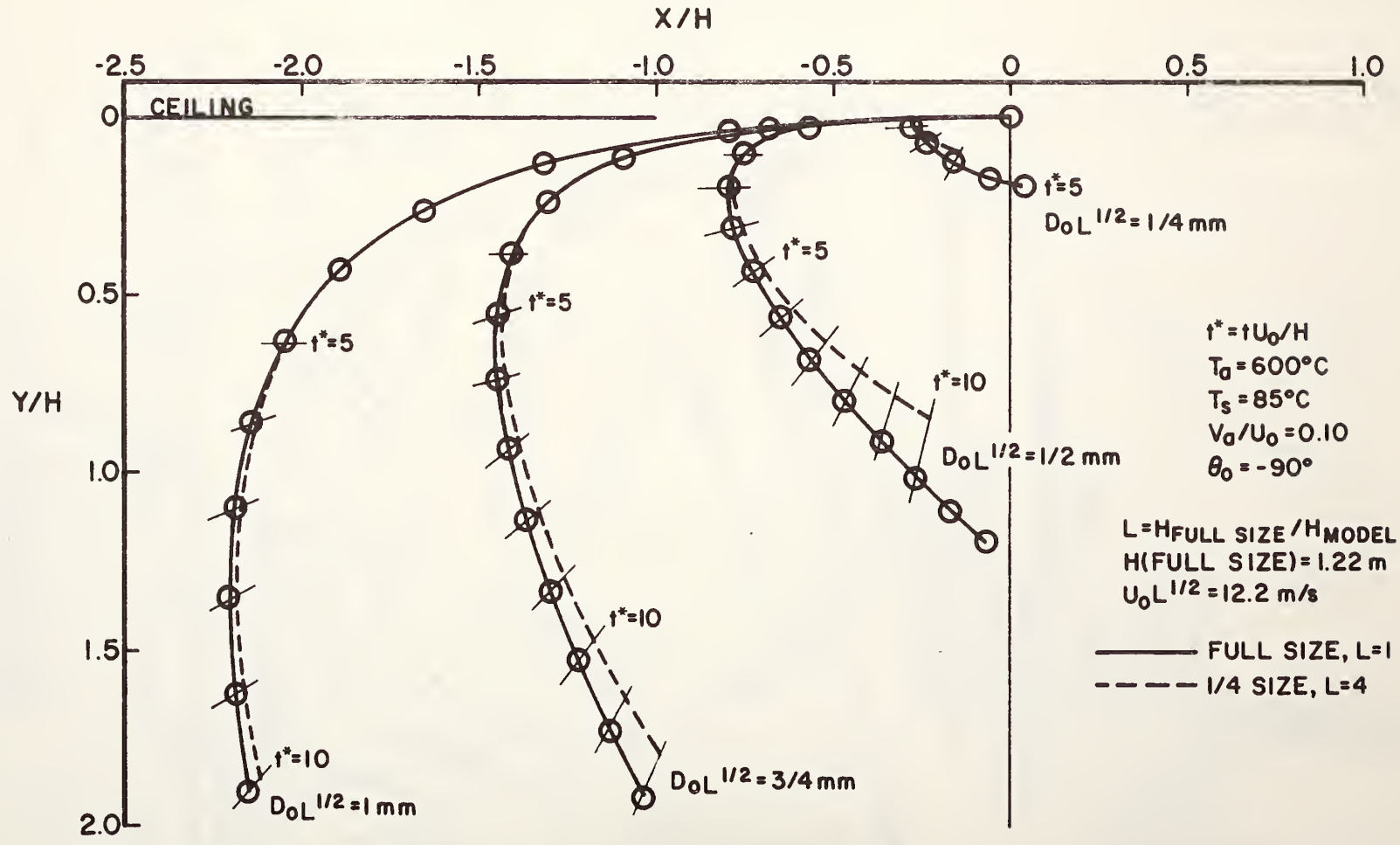

Figure 8. Comparison of Droplet Trajectory Based on Scaling Criteria

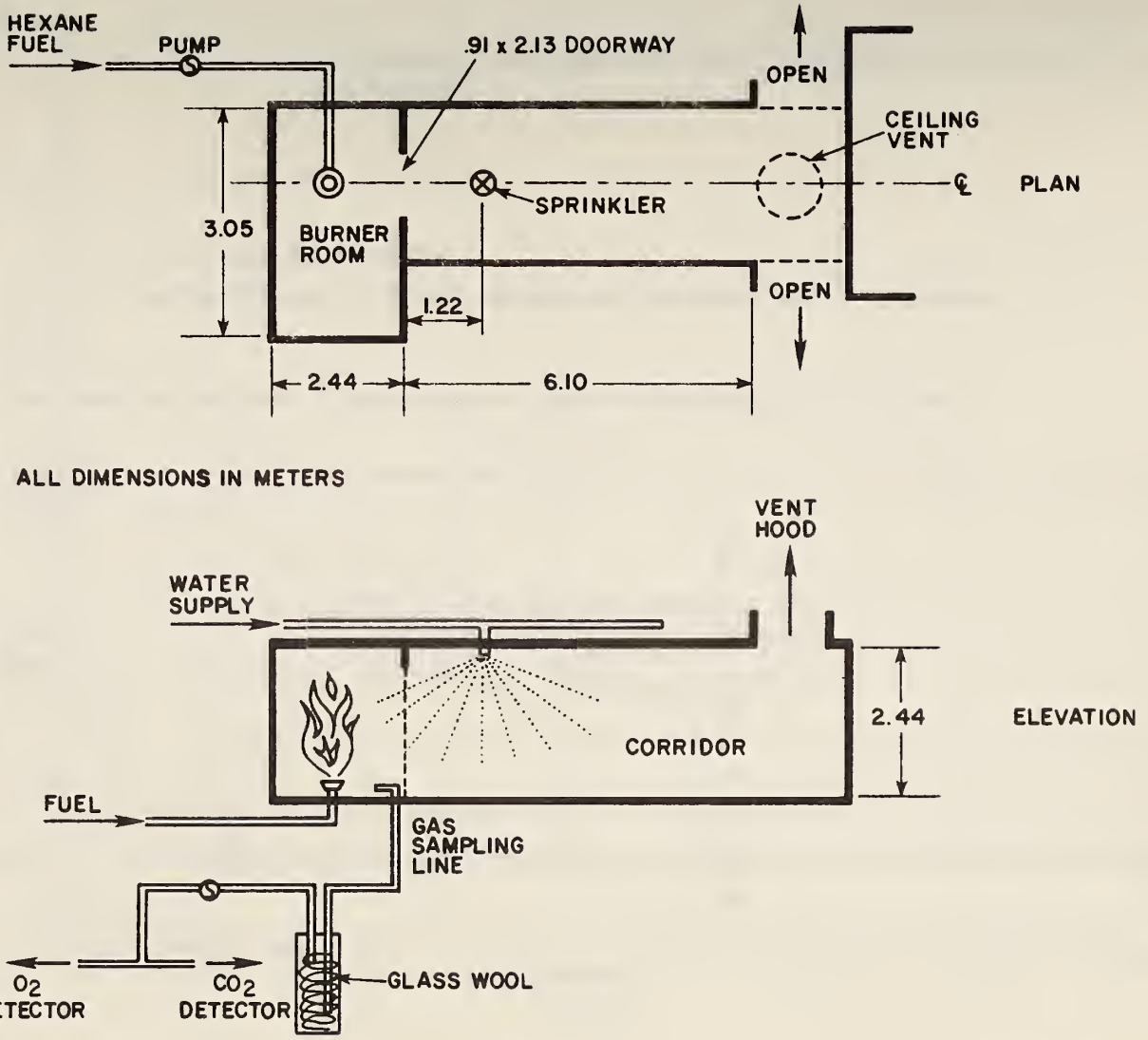

Figure 9. Schematic of Full-Scale Corridor Sprinkler Test Setup

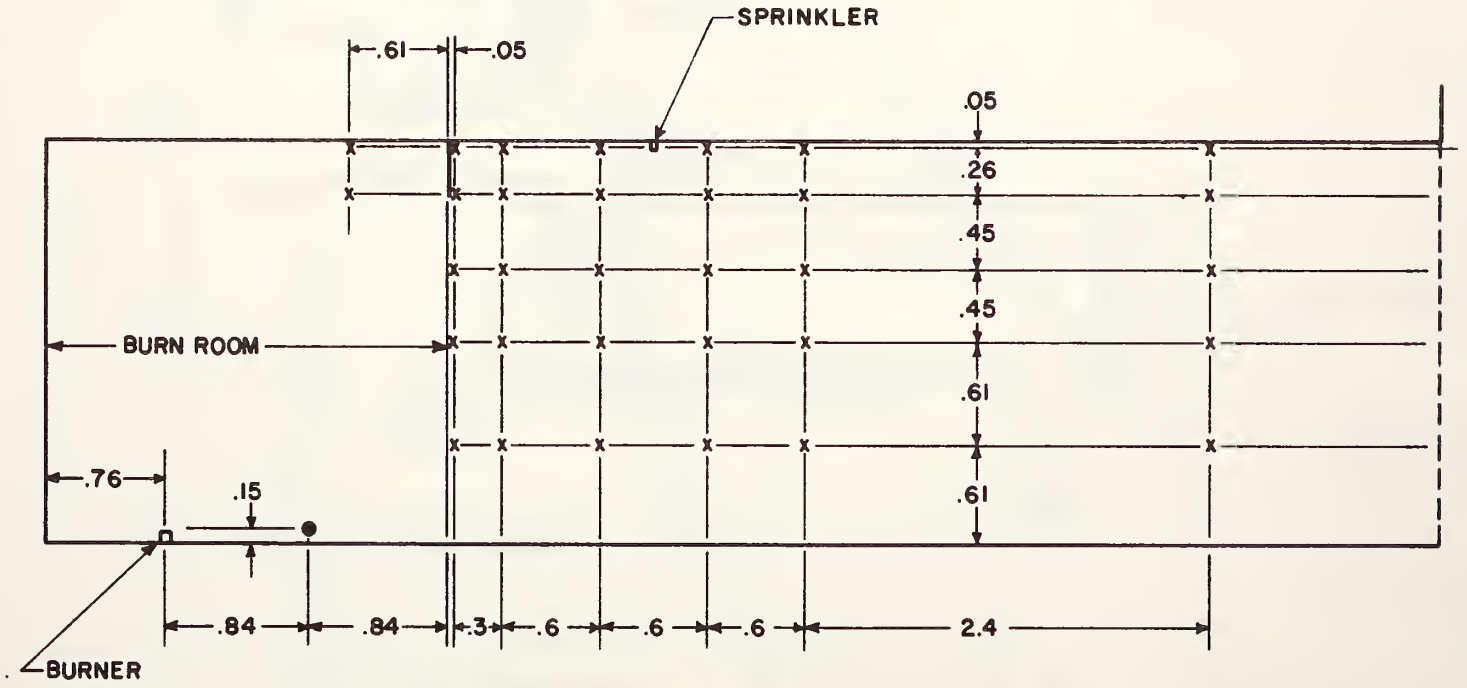

Figure 10. Location of Thermocouples, Gas Sampling Port, and Burner (Full-Scale Test)

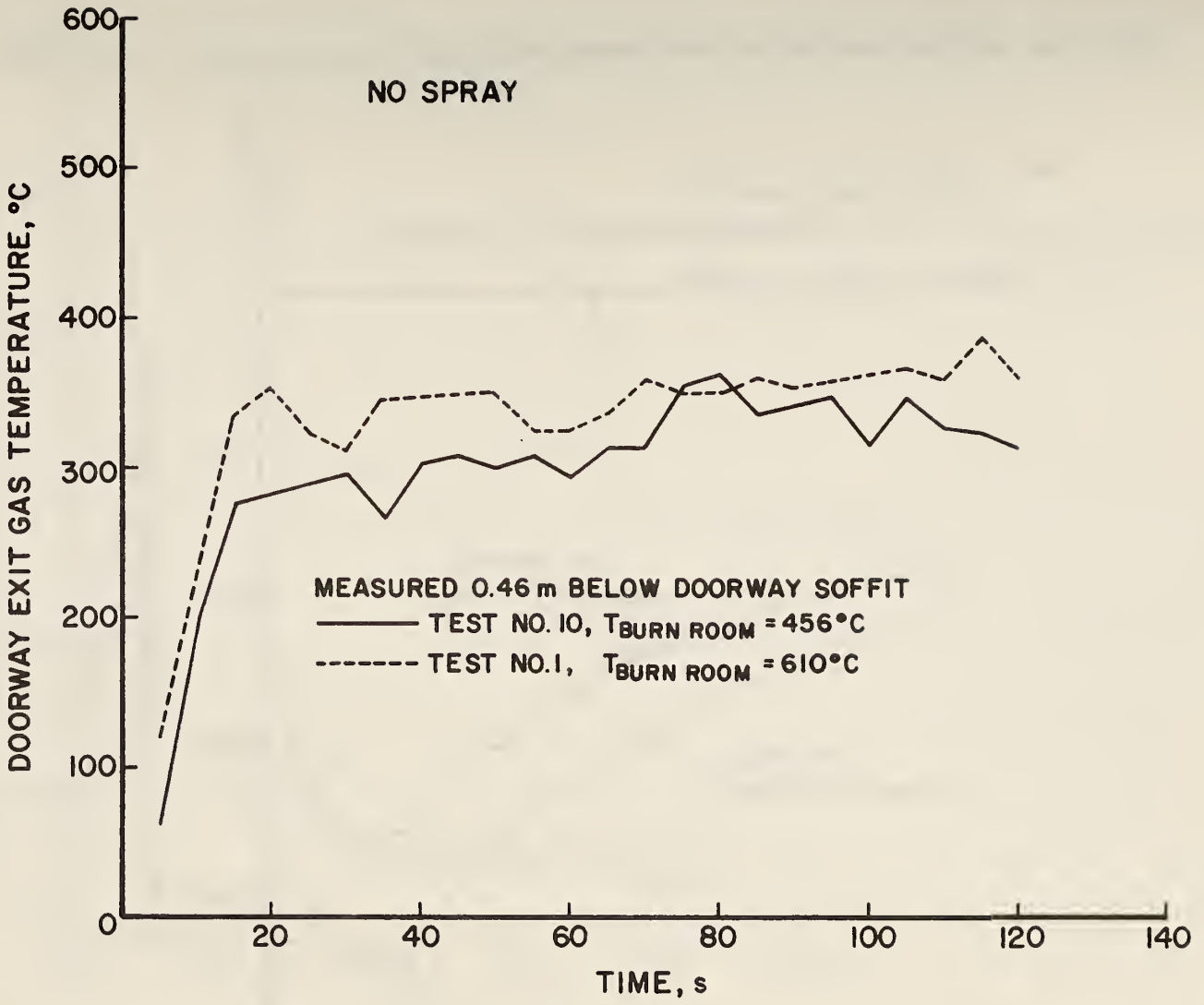

Figure 11. Time History of Exit Gas Temperature at Burn-Room Doorway (No Spray)

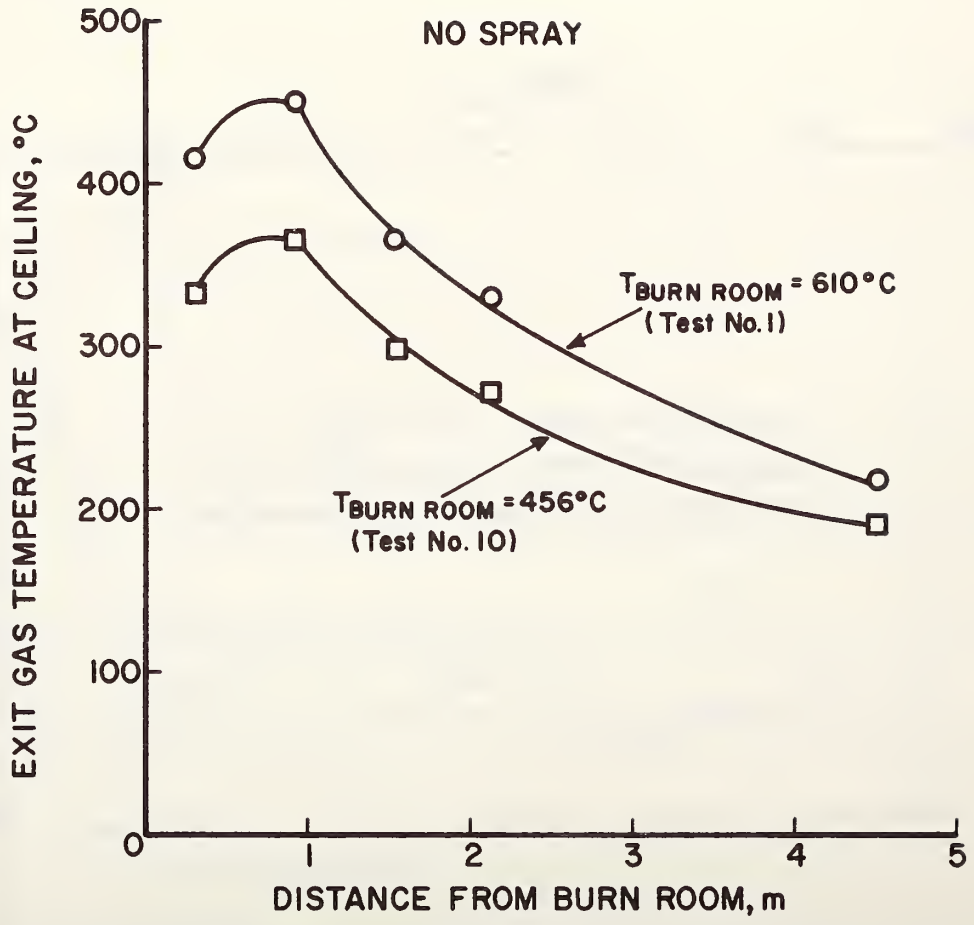

Figure 12. Variations of Ceiling Gas Temperature Along the Corridor (No Spray)

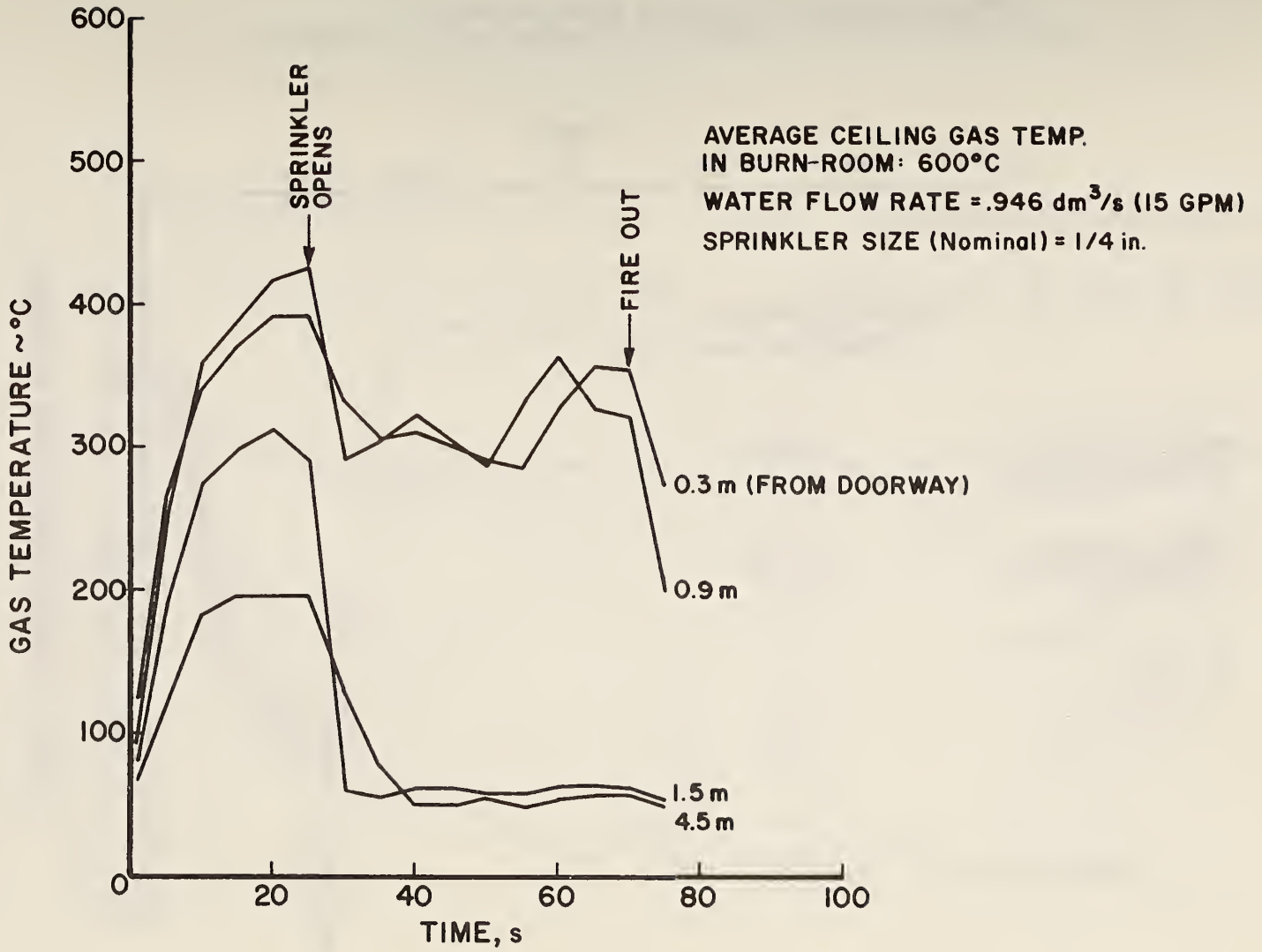

Figure 13. Time History of Corridor Ceiling Gas Temperature (0.05 m below Ceiling)

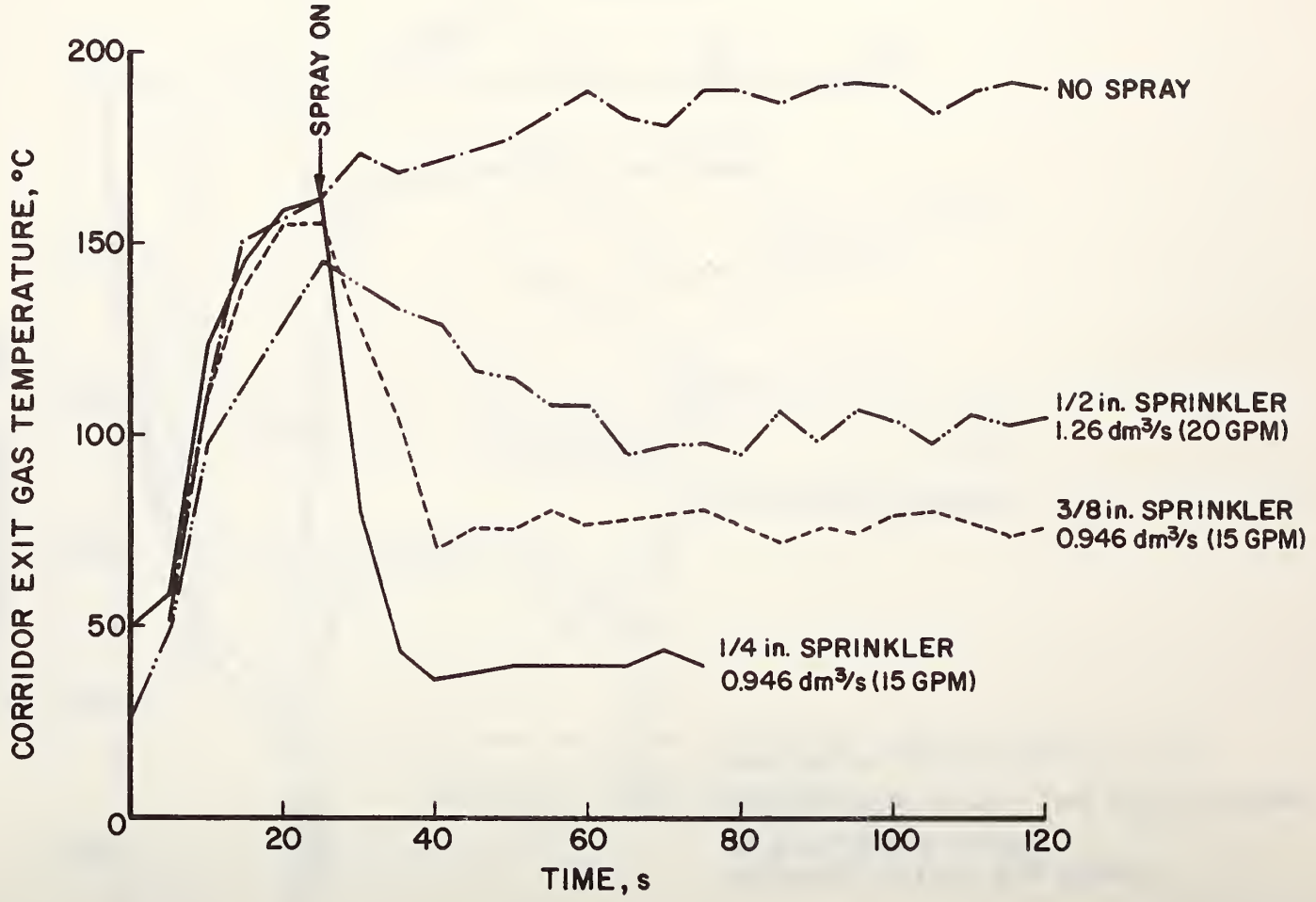

Figure 14. Time History of Corridor Exit Gas Temperature Outside Spray Zone (0.31 m below Ceiling)

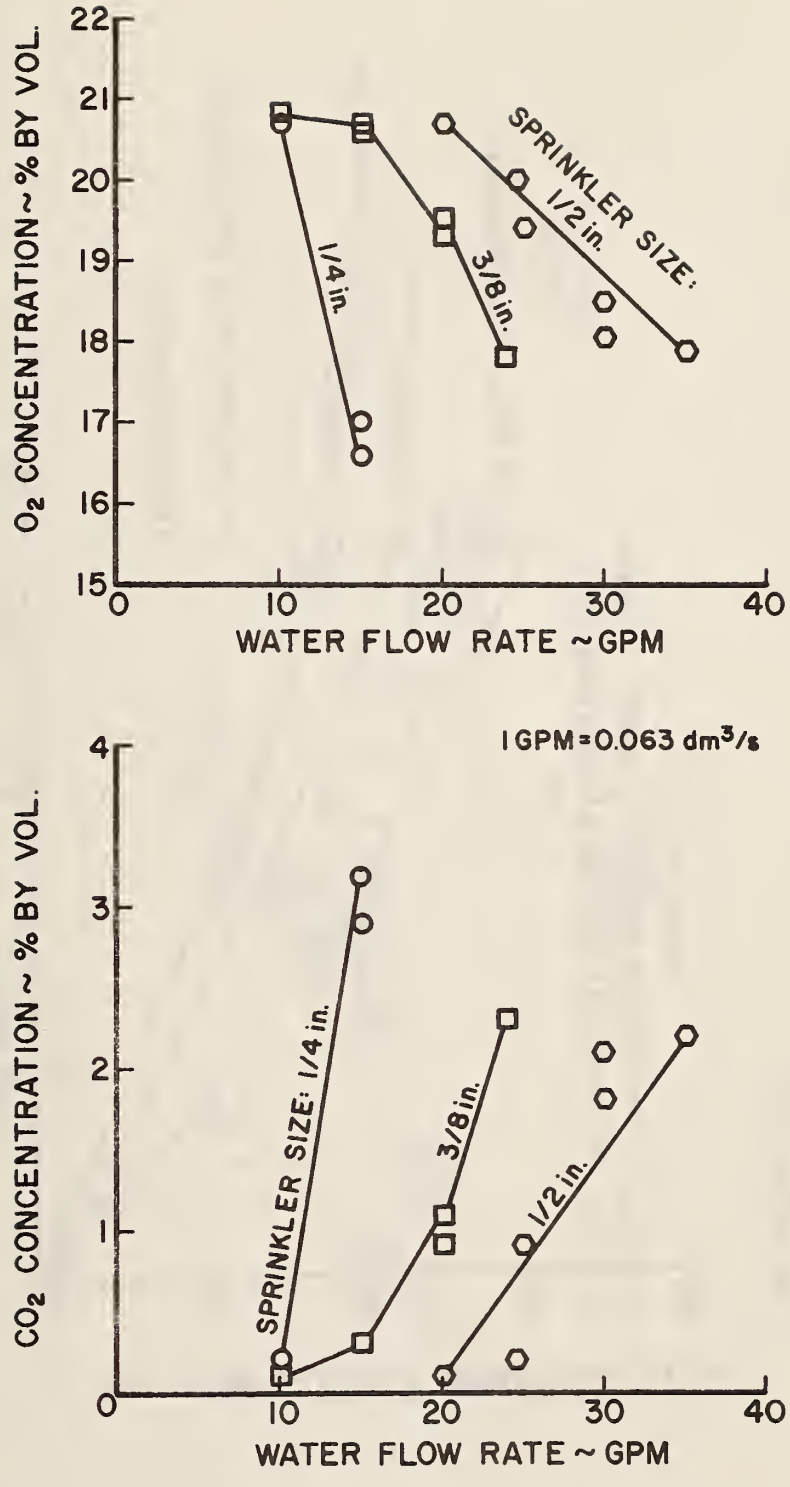

Figure 15. Burner Room O_2 and CO_2 Concentration (Floor Level) Just Before the End of Each Run

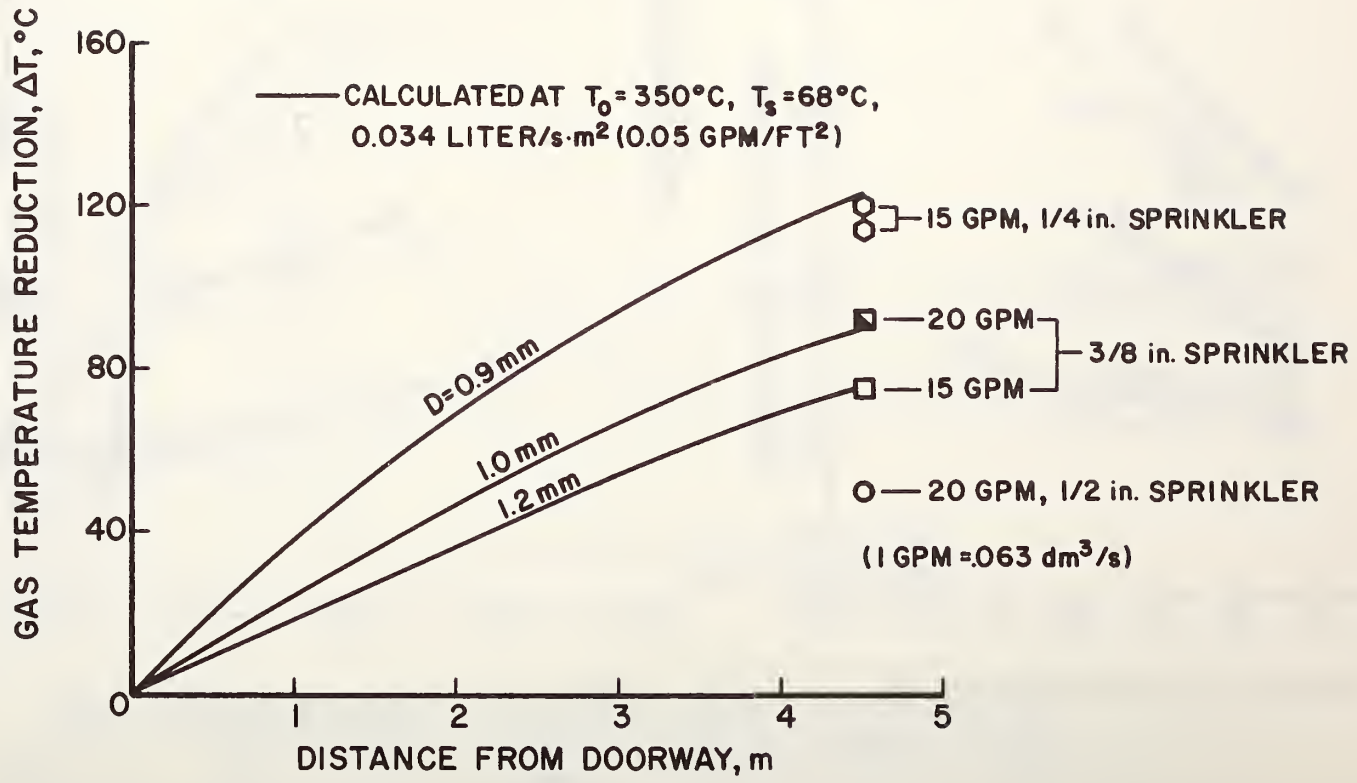

Figure 16. Comparison of Net Corridor Exit Gas Temperature Reduction by Water Spray (Theoretical vs Experimental)

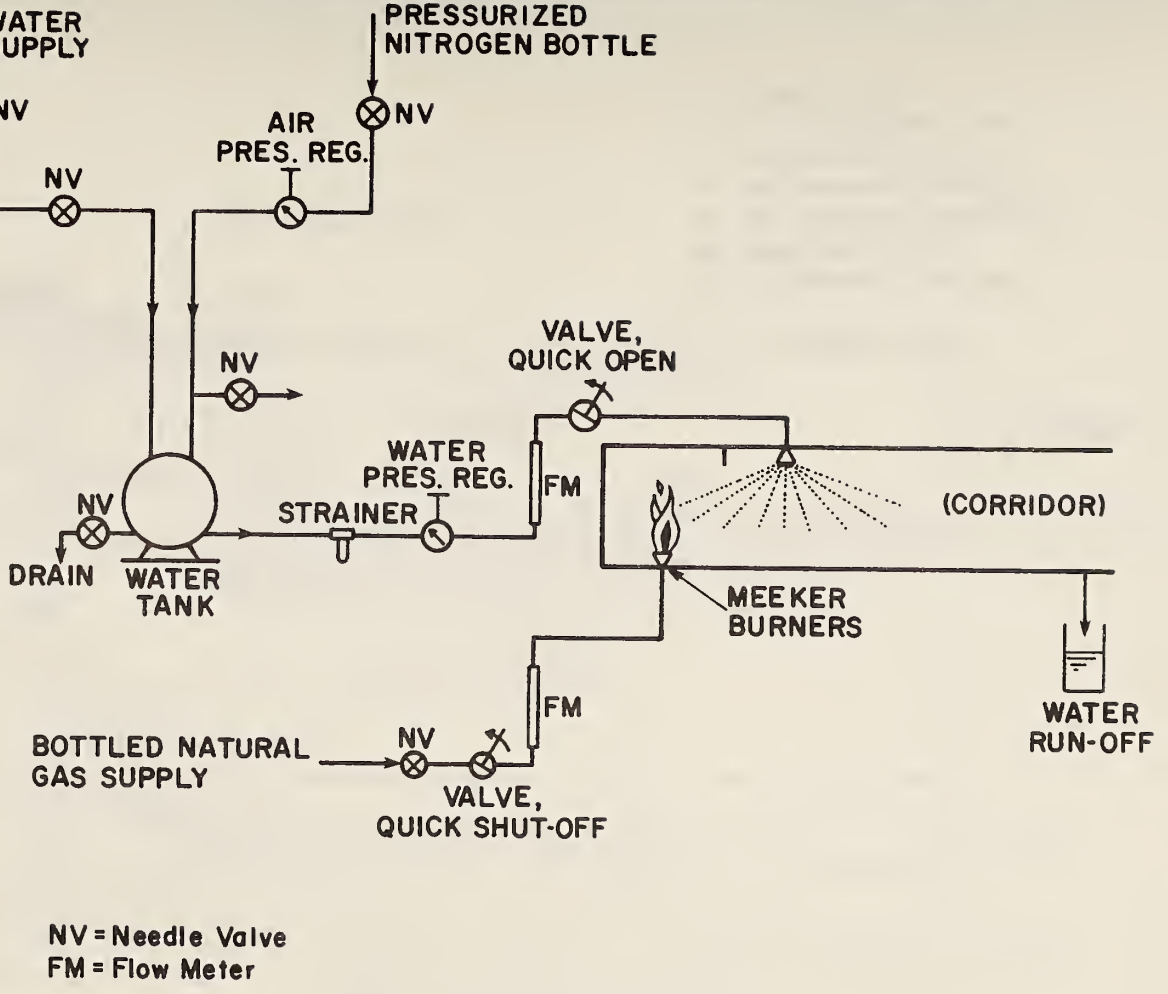

Figure 17. Schematic of One-Quarter Scale Model Experiment Setup

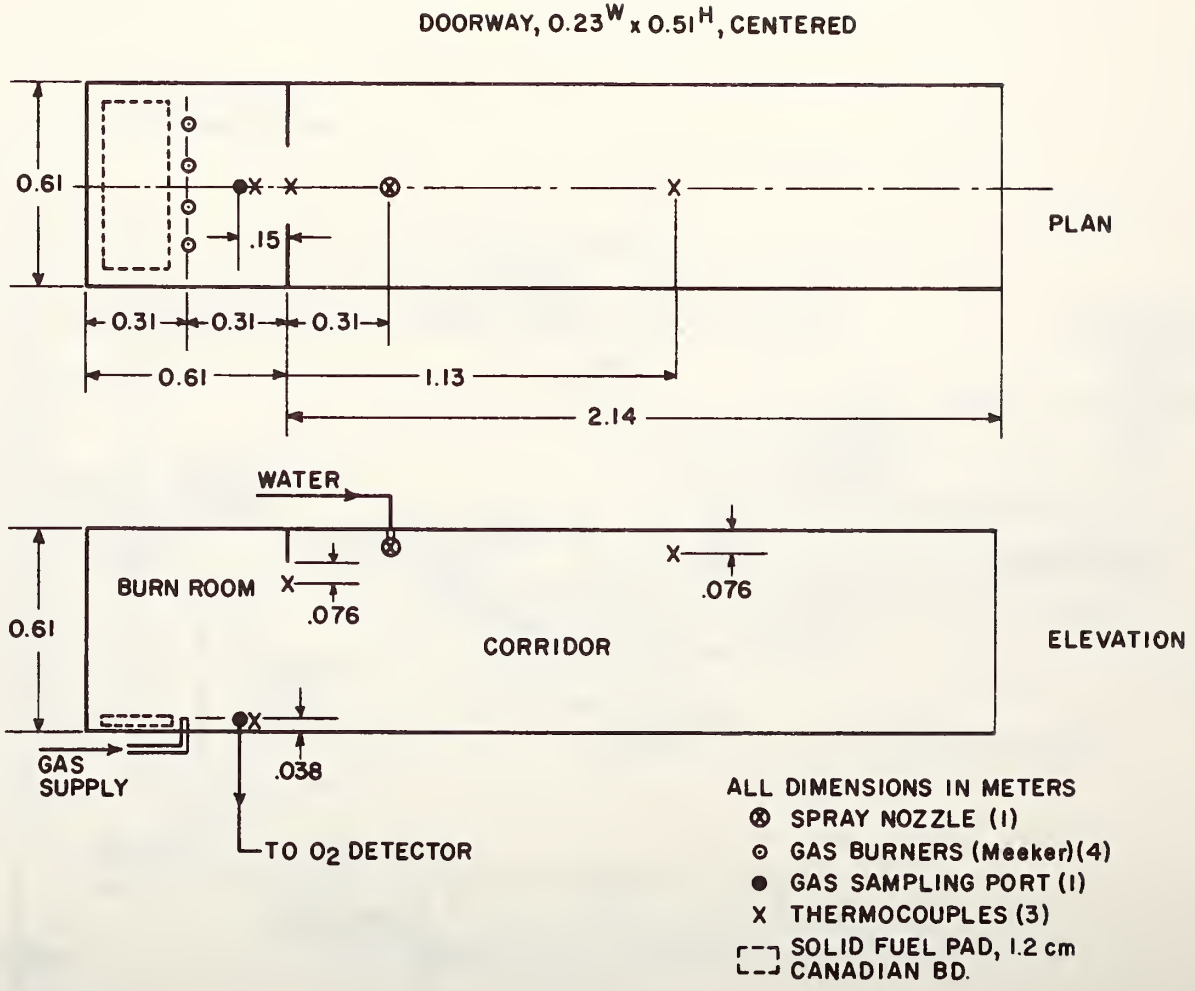

Figure 18. Location of Burners, Thermocouples, Gas Sampling Port, and Fuel Pad (One-Quarter Scale Model)

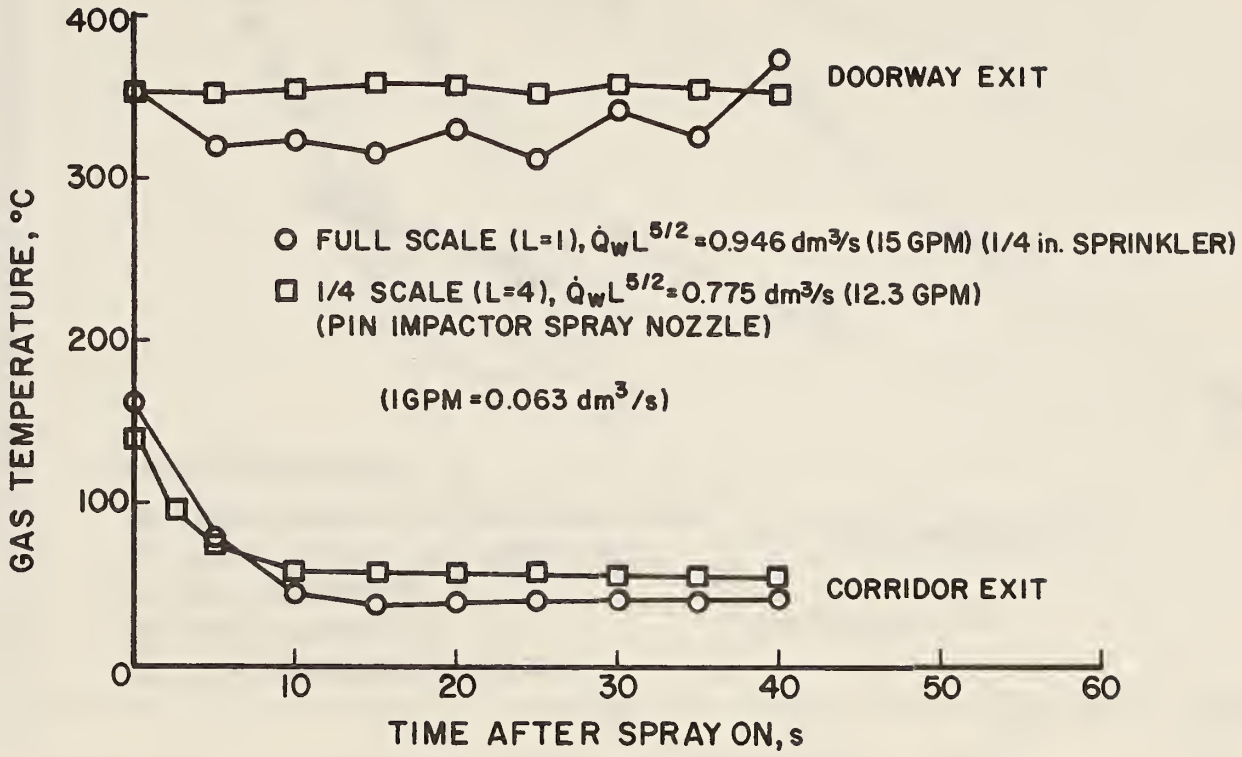

Figure 19. Time History of Corridor Temperature Drop

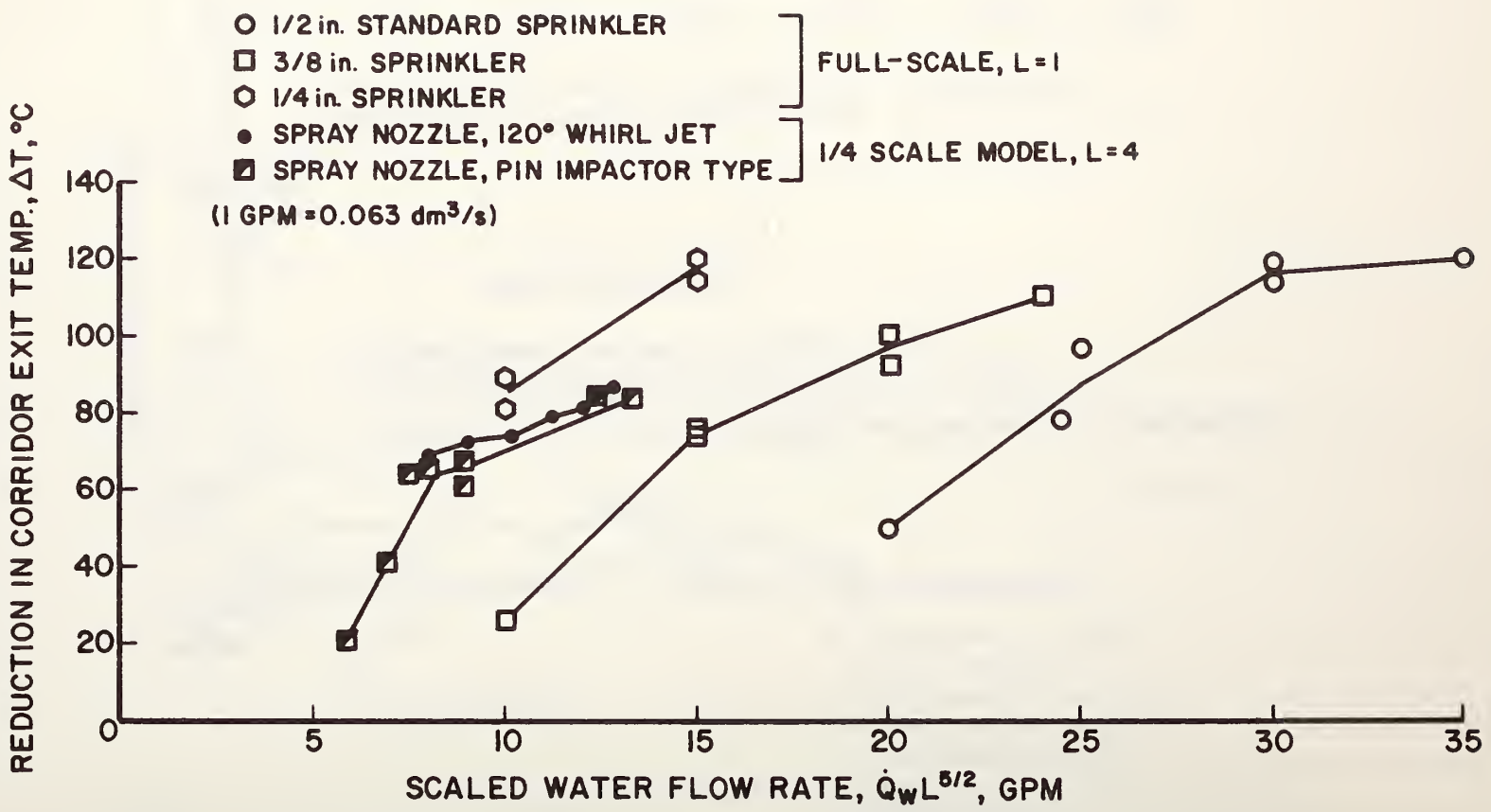

Figure 20. Corridor Exit Temperature Reduction, Full-Scale vs One-Quarter Scale Tests

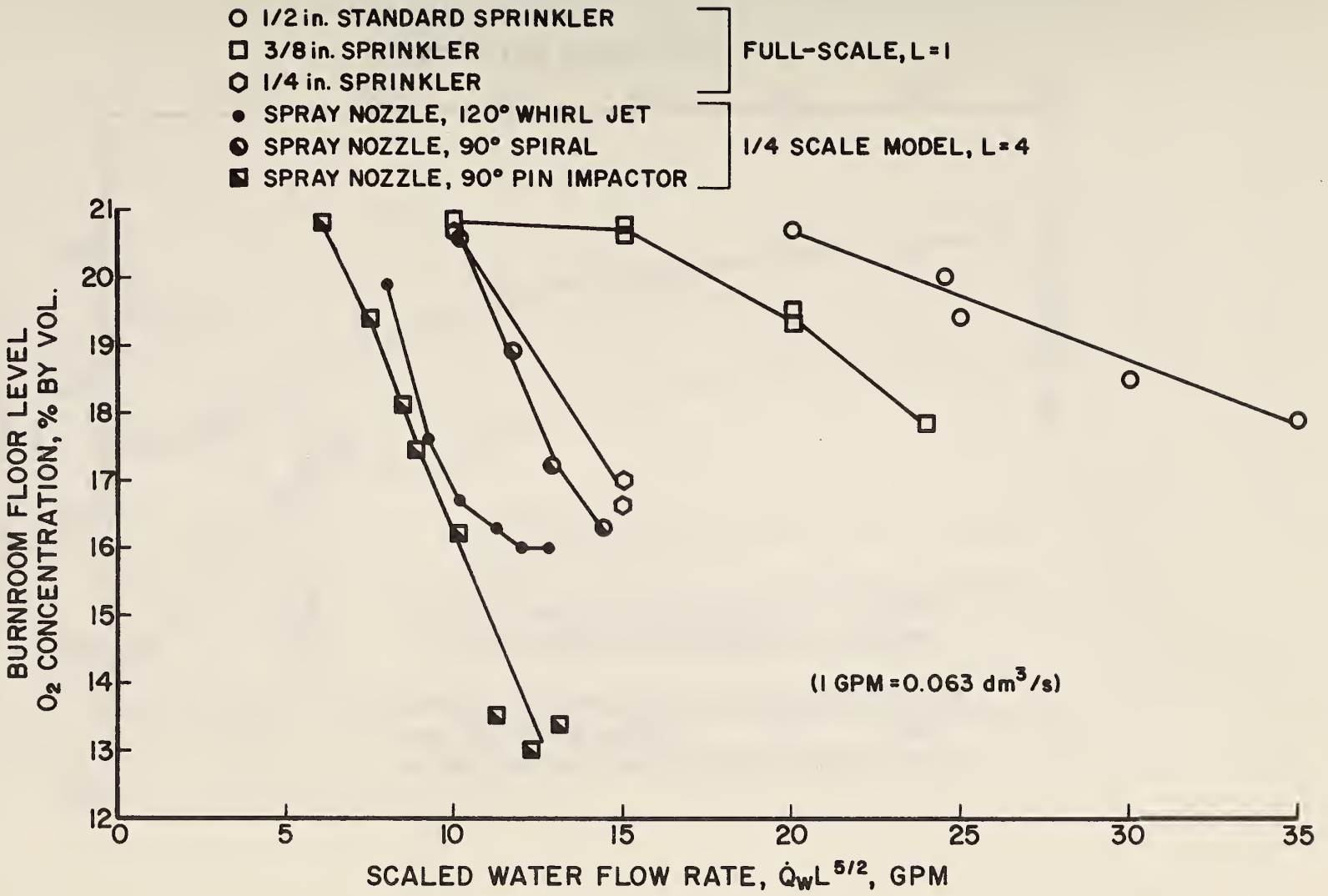

Figure 21. Burn-room Floor Level Oxygen Content, Full-Scale vs One-Quarter Scale Tests

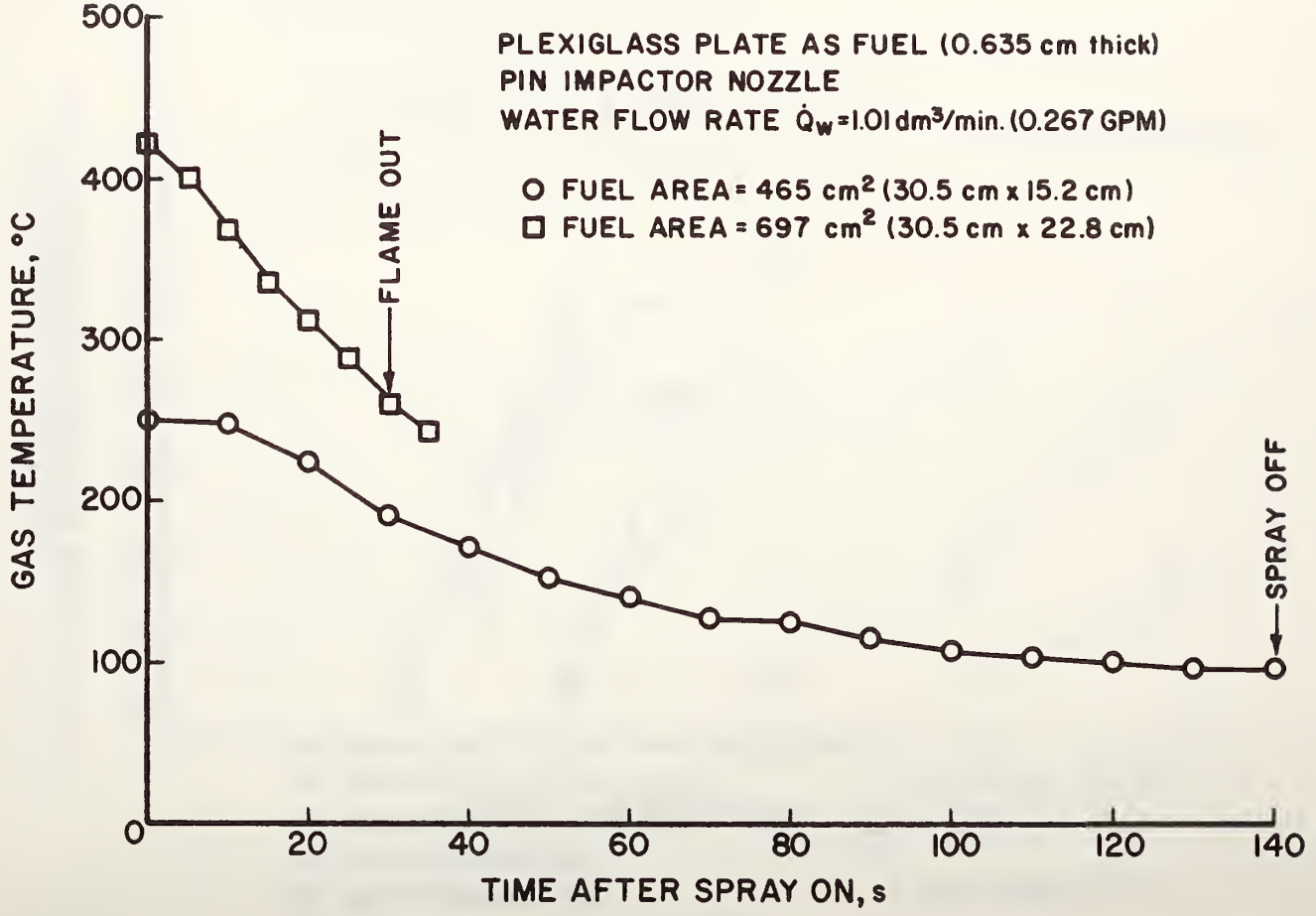

Figure 22. Burn-room Doorway Exit Gas Temperature Variation (Plexiglass Fuel)

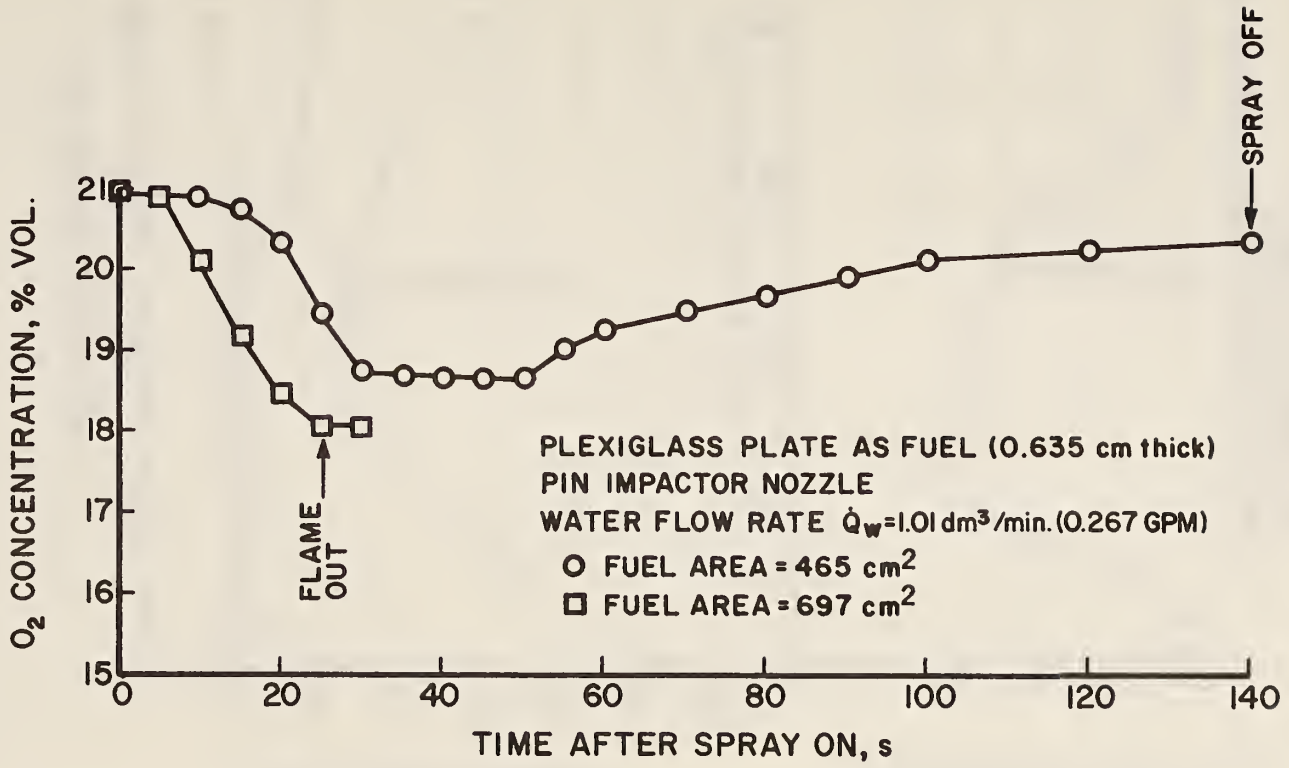

Figure 23. O_2 Content at Burn-room Floor Level (Plexiglass Fuel)

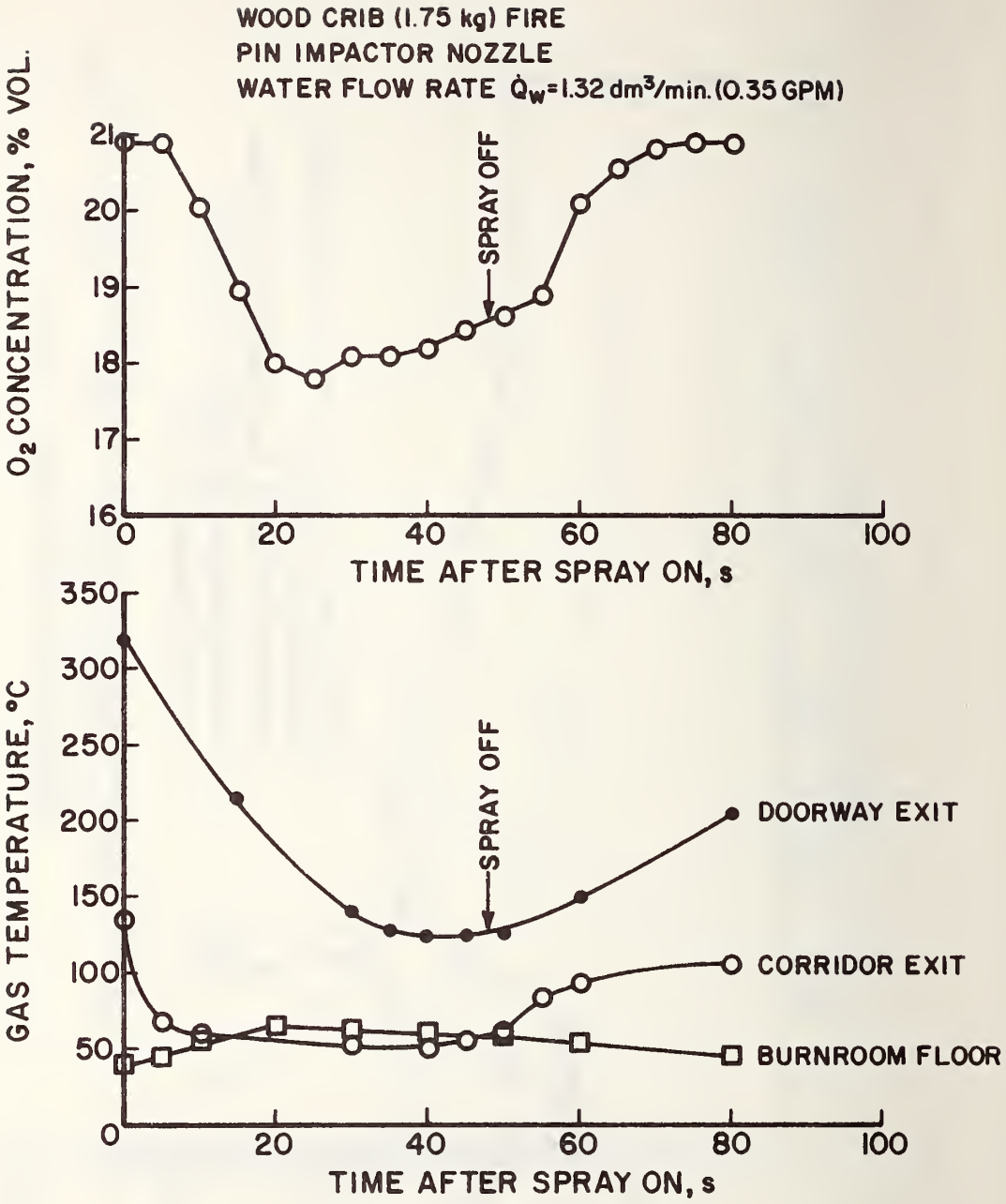

Figure 24. O_2 Content and Gas Temperature Variations (Wood Crib Fuel)

APPENDIX - HEAT TRANSFER BY SPRAY EVAPORATION IN A CROSS FLOW

Referring to figure 1, for a differential control volume dx at x, the mass balance and energy balance equations are, with the assumptions specified in section 2.1:

Mass balance:

$$\frac{d}{dx}\left(\dot{m}_a + \dot{m}_v\right) = \frac{d\dot{m}_v}{dx} = m_w \dot{N} W \qquad \text{(A-1)}$$

where $\dot{m}_a$ = mass flow rate of dry air = constant

$\dot{m}_v$ = mass flow rate of vapor

m_w = mass evaporated per droplet

$\dot{N}$ = Droplet flux density, (No. of drops/sec-unit area)

W = Width of corridor

Energy balance:

$$\frac{d}{dx}\left(\dot{m}_a c_{p_a} T\right) + \frac{d}{dx}\left(\dot{m}_v h_v\right) - m_w \dot{N} h_f W = 0 \qquad \text{(A-2)}$$

where h_v = Enthalpy of vapor at temperature T

h_f = Enthalpy of water at temperature T_s

c_{p_a}, c_{p_v} = Specific heat capacity of air and vapor, respectively

Using $$h_v(T) = h_v(T) - h_v(T_s) + h_v(T_s) = c_{p_v}(T-T_s) + h_v(T_s) \qquad \text{(A-3)}$$

and by definition, the heat of evaporation at temperature T_s is

$$h_{fg}(T_s) = h_v(T_s) - h_f(T_s)$$

eq. (A-2) can be written as:

$$\dot{m}_a c_{p_a} \frac{dT}{dx} + \dot{m}_v c_{p_v} \frac{dT}{dx} + \left[c_{p_v}(T-T_s) + h_{fg}\right] m_w \dot{N} W = 0 \qquad \text{(A-4)}$$

The boundary conditions for eqs. (A-1) and (A-4) are,

$$\text{at } x = 0;$$

$$t = T_o$$

$$\dot{m}_v = 0 \qquad \text{(A-5)}$$

Substituting eq. (A-1) into eq. (A-2) and using eq. (A-3)

$$\frac{d}{dx}\left[\dot{m}_a c_{p_a} T + \dot{m}_v C_{p_v}(T-T_s) + \dot{m}_v h_{fg}\right] = 0$$

Integrating with respect to x and using the boundary condition eq. (A-5),

$$\dot{m}_v = \dot{m}_a c_{p_a}(T_o-T) \Big/ \left[c_{p_v}(T-T_s) + h_{fg}\right] \qquad \text{(A-6)}$$

or,
$$\omega(x) = c_{p_a}(T_o-T) \Big/ \left[c_{p_v}(T-T_s) + h_{fg}\right]$$

where
$$\omega(x) = \dot{m}_v/\dot{m}_a$$

The total heat transferred from hot air to droplets over distance H at droplets velocity V_t is:

$$q = hA(\dot{N}Wdx)\,(T-T_s)\,(H/V_t) = (m_w\dot{N}Wdx)\,h_{fg}$$

which gives

$$m_w = hA\,(H/V_t)(T-T_s)/h_{fg} \qquad \text{(A-7)}$$

where
$$A = \pi D^2 = \text{surface area of a droplet}$$

$$h = \text{heat transfer coefficient from eq. (1), Section 2.1.}$$

Substituting eq. (A-7) and (A-6) into eq. (A-4) gives the differential equation for the temperature of the air-vapor mixture:

$$\dot{m}_a c_{p_a}\left[1 + \frac{c_{p_v}(T_o-T)}{c_{p_v}(T-T_s) + h_{fg}}\right]\frac{dT}{dx} = -\dot{N}WhA(H/V_t)(T-T_s)\left[1 + \frac{c_{p_v}(T-T_s)}{h_{fg}}\right] \qquad \text{(A-8)}$$

Assuming that h, H, V_t, T_s are constant, and defining

$$\theta = (T-T_s)/(T_o-T_s), \quad S = x/W$$

$$B = c_{p_v}(T_o-T_s)/h_{fg}, \quad E = \pi D^2 \dot{N} h W^2 H/(\dot{m}_a c_{p_a} V_t) \tag{A-9}$$

The solution to eq. (A-8) can be written, after simplification, as:

$$\frac{B(\theta-1)}{1+B\theta} - (1+B)\ \ell n\left[\frac{\theta(1+B)}{1+B\theta}\right] = ES \tag{A-10}$$

Also, eq. (A-6) can be written as:

$$\omega = (c_{p_a}/c_{p_v})\ (B)\ (1-\theta) \tag{A-11}$$

Eqs. (A-10) and (A-11) give the solution for the air-vapor mixture temperature T and humidity ratio ω as a function of x.

NBS-114A (REV. 7-73)

U.S. DEPT. OF COMM. BIBLIOGRAPHIC DATA SHEET	1. PUBLICATION OR REPORT NO. NBSIR 77-1287	2. Gov't Accession No.	3. Recipient's Accession No.

4. TITLE AND SUBTITLE

Analytical and Experimental Study of Evaporative Cooling and Room Fire Suppression by Corridor Sprinkler System

5. Publication Date: October 1977

6. Performing Organization Code

7. AUTHOR(S): Stanley T. Liu

8. Performing Organ. Report No.

9. PERFORMING ORGANIZATION NAME AND ADDRESS

NATIONAL BUREAU OF STANDARDS
DEPARTMENT OF COMMERCE
WASHINGTON, D.C. 20234

10. Project/Task/Work Unit No.: 4915679

11. Contract/Grant No.

12. Sponsoring Organization Name and Complete Address (Street, City, State, ZIP)

Same as No. 9

13. Type of Report & Period Covered: Final Report

14. Sponsoring Agency Code

15. SUPPLEMENTARY NOTES

16. ABSTRACT (A 200-word or less factual summary of most significant information. If document includes a significant bibliography or literature survey, mention it here.)

Investigations, both theoretical and experimental, are conducted to evaluate the effects of a corridor sprinkler system on the cooling and suppression of a fire in an adjacent compartment connected by an open doorway. A simplified one dimensional mathematical model is presented to predict the net reduction of the corridor ceiling hot gas temperature by evaporative cooling. Scaling criteria based on the analysis of the motion of an evaporating droplet were developed for the correlation of full-scale and small-scale experimental results and the design requirements of a small-scale experiment. Representative test results from a full-scale and a one-quarter scale model experiments are presented. These tests demonstrate the effectiveness of water spray in reducing the corridor hot gas temperature to a level low enough for safe passage, and in causing a strong recirculating flow at the room doorway. This flow reduces the oxygen content around the fire significantly, and results in a much reduced burning rate of the fuel. The effect of the spray droplet size on the cooling and on fire suppression is discussed.

17. KEY WORDS (six to twelve entries; alphabetical order; capitalize only the first letter of the first key word unless a proper name; separated by semicolons) Automatic sprinklers; compartment fire; corridor sprinkler systems; droplet size; droplet trajectory; evaporative cooling; fire suppression; full-scale test; gas temperature; oxygen content; recirculating flow; reduced scale model test; scaling criteria; spray water flow rate; water spray.

18. AVAILABILITY

[X] Unlimited

[ ] For Official Distribution. Do Not Release to NTIS

[ ] Order From Sup. of Doc., U.S. Government Printing Office Washington, D.C. 20402, SD Cat. No. C13

[X] Order From National Technical Information Service (NTIS) Springfield, Virginia 22151

19. SECURITY CLASS (THIS REPORT)	21. NO. OF PAGES
UNCLASSIFIED	56
20. SECURITY CLASS (THIS PAGE)	22. Price
UNCLASSIFIED	$5.25

USCOMM-DC 29042-P74